Columbia University

A search for new diboson resonances in the boosted semi-leptonic final state at $\sqrt{s} = 13$ TeV with the ATLAS detector

Ryne Carbone
Columbia University

Thesis Defense
New York, NY

Wednesday 27th September, 2017

Outline

Physics Beyond the Standard Model (BSM)

- Standard Model (SM) describes physics well up to TeV-scale, but incomplete (dark matter, neutrino masses, matter-antimatter asymmetry, etc.)

Open Issues

- Fine tuning of Higgs mass
  - Loop correction to Higgs mass proportional to scale of new physics ($\Delta m_H^2 \propto \Lambda_{\mathrm{cutoff}}^2$)
  - Incredible fine tuning, expect $\Lambda_{\mathrm{cutoff}} \sim \Lambda_{\mathrm{Planck}} \sim 10^{19}$ GeV, $m_H \simeq 10^2$ GeV
- Minimal Higgs sector (in SM)
  - One complex scalar doublet addresses two disparate issues:
    1) Generate weak boson masses while retaining gauge invariance
    2) Generate fermion masses
- EW and Strong sectors commute
  - Unsatisfying – larger symmetry group driving unification at larger scale?
- SM does not include gravity

Diboson Resonances

Searching for Resonances

- Many BSM theories predict massive boson resonances to address limitations of SM
- Can be searched for at Large Hadron Collider (LHC)
  - Proton collisions can produce resonances through variety of processes
- Different models predict resonances with different spins
- Couplings to SM gauge bosons (decay to a pair)
- Look at semi-leptonic decay mode (WV for $V = \{W, Z\}$)
  - Leptonic decay ($W \to \ell\nu$ for $\ell = \{e, \mu\}$, BR 21 %): clean reconstruction in hadron collider
  - Hadronic decay ($V \to q\bar{q}'$ for $q, q' = \{u, d, c, s, b\}$, BR$\sim 70\,\%$): large branching ratio

Neutral Heavy Higgs (Spin-0)

- Representative of theories with extended Higgs sector
  - Address minimal SM Higgs sector with multiple copies of the SM complex scalar doublet
  - In simplest two Higgs doublet model, two neutral scalars (one SM-like, one heavy), one neutral pseudo-scalar, and two charged scalars predicted
- gluon-gluon fusion (ggF) production dominant (through quark loop)
- Vector boson fusion (VBF) production also considered
  - Incoming quarks radiate vector bosons
  - Quarks hadronize, form jets with small deflection

Production	Diagram
ggF	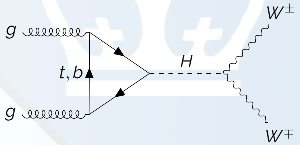
VBF	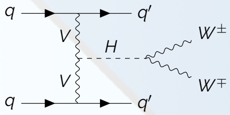

- Modeling choices:
  - Narrow width approximation (NWA), width less than detector resolution
  - Neglect interference with SM diboson production

I. P. Ivanov, Prog. Part. Nucl. Phys. 95 (2017) 160-208.
V. Barger et al., Phys. Rev. D 77 (2008) 035005.

Heavy Vector Triplet (HVT) (Spin-1)

- Phenomenological Lagrangian with parameters that determine mass and relevant couplings of resonance
- g_V: strength of new interaction
- c_F, c_H: deviation from unity of HVT coupling to fermions, and SM gauge bosons and Higgs
- SM weak boson coupling $\propto g_V c_H$ fermionic coupling $\propto g^2 c_F / g_V$
- c_F taken to be universal and ~ 1

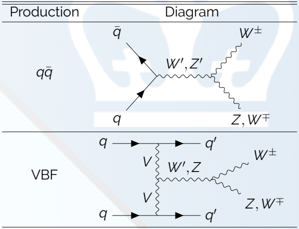

- quark-antiquark fusion (qqF) production dominant, however if $c_F \simeq 0$, VBF is significant $\rightarrow$ both mechanisms considered

Model-A: $g_V = 1$, $c_H \simeq g^2/g_V$

- Characterizes theories with extended gauge groups
- Fermions and SM gauge bosons have comparable couplings

Model-B: $g_V = 3$, $c_H \simeq 1$

- Characterizes theories of strongly interacting composite Higgs sector (address fine-tuning problem)
- Fermionic coupling suppressed

D. Pappadopulo, A. Thamm, R. Torre, and A. Wulzer, JHEP 09 (2014) 60

Randall-Sundrum (RS) Bulk Graviton (Spin-2)

$$ds^2 = e^{-2\kappa r_c|\phi|}\eta_{\mu\nu}dx^\mu dx^\nu + r_c^2 d\phi^2$$

- Theory of a warped extra dimension
  - Gravity and SM fields (except Higgs field) can propagate in bulk of extra dimension (extension of original theory)
  - Gravity strong on (3+1)-dim "Planck"-brane
  - Separated in bulk from "TeV"-brane
- Localization of SM fields in bulk reproduces flavor hierarchy on TeV-brane
  - Lighter particles on TeV-brane localized closer to Planck-brane, larger warping factor
  - RS bulk graviton realized on TeV-brane as first Kaluza Klein excitation, G^*
  - Coupling of graviton excitation to W_L/Z_L enhanced by localization of Higgs field on TeV-brane
- κ: curvature scale of new dim.
  - Cannot be much larger than Planck scale for theory to remain perturbative
  - Consider values $\kappa/\overline{M}_{\mathrm{Pl}} = 1.0, 0.5$
  - $\overline{M}_{\mathrm{Pl}} = M_{\mathrm{Pl}}/\sqrt{8\pi}$ is reduced Planck mass

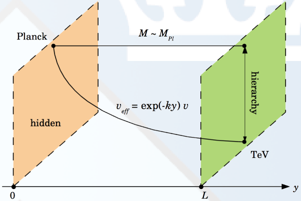

- Dominant production mechanism is ggF

Production	Diagram
ggF	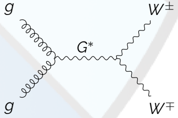

K. Agashe, H. Davoudiasl, G. Perez, and A. Soni, Phys. Rev. D 76 (2007) 036006

CERN Large Hadron Collider (LHC)

- 26.7 km *pp* collider in Geneva, Switzerland
- Center-of-mass energy $\sqrt{s} = 13$ TeV (currently)
- 400 MHz RF cavities produce 25 ns proton "bunch" spacing, $\sim 1.5 \times 10^{11}$ *p*/bunch

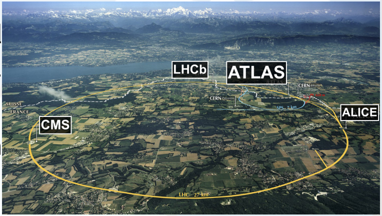

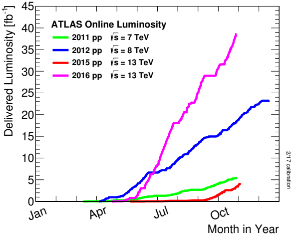

- Total data (2015+2016): $\int \mathcal{L} = 36.1$ fb^{-1}
  $\mathcal{L}_{\text{peak}} = 1.37 \times 10^{34}$ cm^{-2}s^{-1} (nominal 10^{34} cm^{-2}s^{-1})

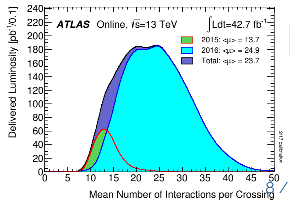

- Pileup: high instantaneous luminosities create multiple interactions per crossing, μ
- $\langle \mu \rangle = 24.9$ in 2016 $\rightarrow$ challenging environment!

ATLAS Detector

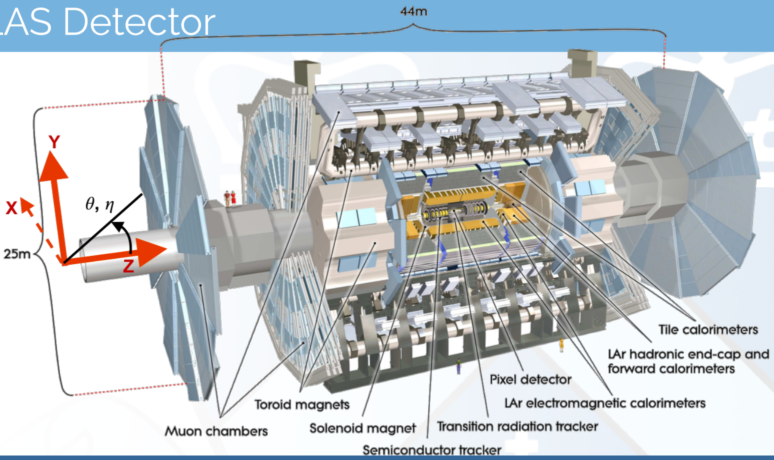

Cylindrical Coordinate System

- Beamline along $\hat{z}$, ϕ measured about beamline from $\hat{x}$, θ measured from $\hat{z}$
- Pseudo-rapidity: $\eta = -\ln(\tan\theta/2)$ (massless or highly relativistic limit, $\Delta\eta$ invariant under Lorentz boosts in $\hat{z}$, useful at LHC where collisions have varying boosts in lab frame)
- $\Delta R = \sqrt{(\Delta\phi)^2 + (\Delta\eta)^2}$

Particles in ATLAS

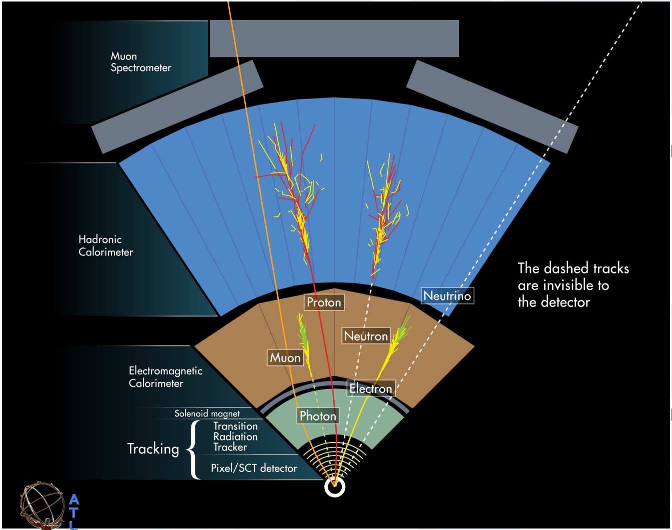

- Inner Detector: (ID) charged particle tracking, vertex reconstruction, short-lived particles
- Calorimeters: fully contain and measure energy from electromagentic and hadronic activity (e, γ, hadrons), measure missing transverse energy ($E_{\mathrm{T}}^{\mathrm{miss}}$)
- Muon Spectrometer: (MS) muons escape calorimeter, precise tracking for high-p_{T} regime

Leptons and $E_{\mathrm{T}}^{\mathrm{miss}}$

- Electrons:
  - Sliding window algorithm finds local maxima of clustered energy deposits in EM calorimeter
  - "Calo-clusters" matched to ID tracks
- Muons:
  - MS tracks extrapolated and matched to ID tracks
- Identification
  - Combination of tracking and calorimeter variables to identify "signal" leptons
- Isolation
  - Track and/or calorimeter-based cuts select "signal" leptons with small amount of nearby energy deposits

Missing Transverse Energy ($E_{\mathrm{T}}^{\mathrm{miss}}$)

- Identified with neutrinos
  - No energy deposits in calorimeters
  - No tracks in ID or MS
- $E_{x(y)}^{\mathrm{miss}} = -\sum_{e \in \{\mathrm{electrons}\}} p_{x(y)}^{e} - \sum_{\mu \in \{\mathrm{muons}\}} p_{x(y)}^{\mu} - \sum_{j \in \{\mathrm{jets}\}} p_{x(y)}^{j} - \sum_{s \in \{\mathrm{soft\ terms}\}} p_{x(y)}^{s}$

  $E_{\mathrm{T}}^{\mathrm{miss}} = \sqrt{(E_x^{\mathrm{miss}})^2 + \left(E_y^{\mathrm{miss}}\right)^2}$

  "Soft terms" correspond to ID tracks not matched to reconstructed objects

Jets

- Collimated spray of hadrons
  - Due to quarks from hard-scatter event, or decay of subsequent unstable particles ($W/Z \to q\bar{q}'$)
  - Color confinement causes hadronization of isolated quarks or gluons
- Match clustered (anti-k_{T} algorithm) topologically connected calorimeter energy deposits to ID tracks
- Two types of jets used in this search:
  - Small-R jets ($R = 0.4$): used to identify jets from b-hadron decays, or jets from VBF interactions
  - Large-R jets ($R = 1.0$): used to identify jets from hadronically decaying W/Z bosons

Anti-k_{T} Clustering Algorithm

- Sequential recombination algorithm
- R: distance parameter $\sim$ size of jet
- Clusters highest p_{T} constituents first
- Roughly conical jets

b-tagging

- Multivariate algorithm
- Accounts for impact parameter, secondary vertex reconstruction, full decay chain reconstruction

Large-R Jets ($R = 1.0$)

Trimming

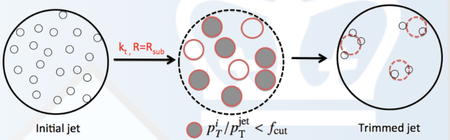

- Recluster into sub-jets (anti-k_{T}, $R = 0.2$)
- Remove if $p_{\mathrm{T}}^{\mathrm{subjet}} < 0.05 p_{\mathrm{T}}^{J}$

Jet Substructure ($D_2^{\beta=1}$)

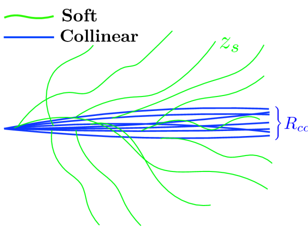

- Two-body decays of vector bosons have jet substructure
- Typically absent from hadronization of gluons and light quarks

Boson Tagging

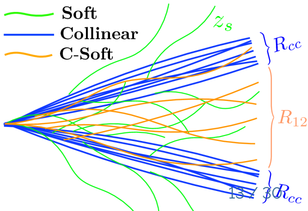

- Identify hadronically decaying W/Z bosons
- Fixed efficiency working points (50 % and 80 %)
- Tagging based on:
  - Jet substructure, $D_2^{\beta=1}$ (upper cut)
  - Jet mass (window cut)

Boosted Regime

- For high resonance masses, each daughter boson will have transverse momentum equal to approx. half resonance mass (Eq. 1)
- Quark separation $\Delta R(q,\bar{q}')$ if boson decays hadronically described by Eq. 2

$$p_{\mathrm{T}}(V) \simeq m(WV)/2 \qquad (1)$$

$$\Delta R(q,\bar{q}') \simeq 2m(V)/p_{\mathrm{T}}(V) \qquad (2)$$

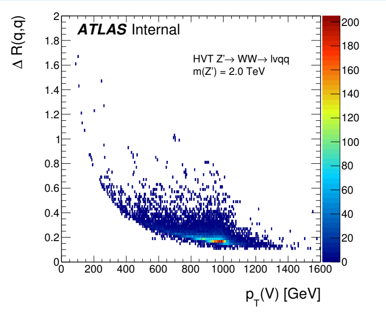

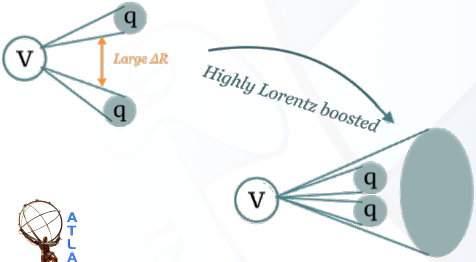

- If small separation (ΔR), small-R jet ($R = 0.4$) cannot separately resolve decay products (degraded energy resolution)
- Use large-R jet ($R = 1.0$) to instead fully capture decay
- Boosted regime $\Rightarrow$ $m(WV) > 500$ GeV, $p_{\mathrm{T}}(V) \geq 200$ GeV

Resonant Production of SM Weak Bosons ($WV \to \ell\nu qq$)

- Look for high resonance masses, bosons in decay will be boosted
- W decays leptonically ($W \to \ell\nu$)
  - Reconstruct as lepton (e, μ), and $E_{\mathrm{T}}^{\mathrm{miss}}$ (ν)
  - Impose W mass constraint on lepton-$E_{\mathrm{T}}^{\mathrm{miss}}$ system
- V (W/Z) decays hadronically
  - Reconstruct collimated quark pair as large-R jet denoted by J
- Look for excesses in invariant mass distribution of the lepton, $E_{\mathrm{T}}^{\mathrm{miss}}$, large-R jet system above SM background prediction

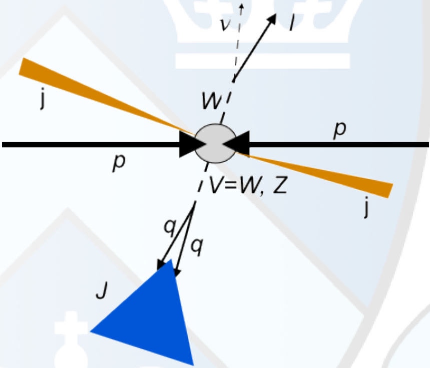

- Classify event by production mechanism
  - If two small-R jets present, consistent with VBF production
  - Otherwise classify as ggF or qqF production

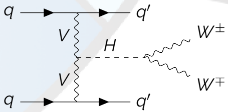

Standard Model Background Processes

- SM processes can mimic final state: lepton (e, μ), $E_{\mathrm{T}}^{\mathrm{miss}}$, large-R jet
- Bkg. processes simulated with Monte Carlo (MC).

- W+jets: production of W (decays leptonically) in association with quarks or gluons
  - Quarks/gluons hadronize, reconstructed as one or more jets
  - Jets lack substructure seen in hadronic decay of W/Z
  - Jets usually lower masses

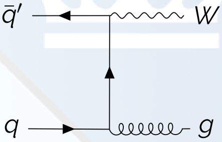

- $t\bar{t}$: each top decays to Wb (BR nearly 1), one W decays leptonically.
  - Distinguished by presence of additional b-jets in final state
  - $b-$ quark can also be reconstructed inside large-R jet

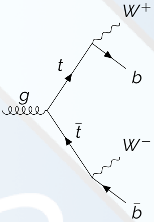

Normalization of these two main backgrounds, W+jets and $t\bar{t}$, constrained by dedicated control regions and determined in statistical fit.

Standard Model Background Processes

Also consider additional minor backgrounds

- Single-t: also produce additional b-jets in final state

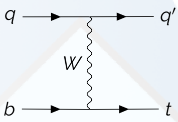

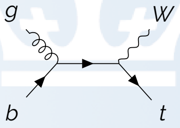

- Z+jets: (decays leptonically to $Z \to \ell\ell$) One lepton must be incorrectly reconstructed $\to$ reducible background, impose strict requirement on number of leptons

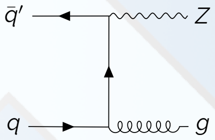

- SM diboson: two weak bosons produced with non-resonant mass spectrum

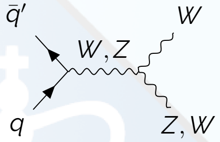

Contribution from non-resonant QCD production of multiple jets (fake lepton reconstructed) determined to be negligible

Event Selection

- Production Mechanism: "VBF selection" if two additional small-R jets, else "ggF selection"
- One lepton: (e, μ)
  - $p_{\mathrm{T}} > 27$ GeV
  - $|\eta| < 2.5$
- 1 Large-R jet
  - no overlap with VBF jets ($\Delta R(j, J) > 1.5$)
  - $p_{\mathrm{T}}(J) > 200$ GeV
  - $m(J) > 50$ GeV
  - $|\eta| < 2.0$
- Multi-jet Rejection:
  - $E_{\mathrm{T}}^{\mathrm{miss}} > 100$ GeV
  - $E_{\mathrm{T}}^{\mathrm{miss}}/p_{\mathrm{T}}(W \to e\nu) > 0.2$
- Boosted Regime: $p_{\mathrm{T}}(W \to \ell\nu) > 200$ GeV
- Momentum Balance: Weak bosons should have momentum equal to approx. half resonance mass.
  - $p_{\mathrm{T}}(W \to \ell\nu)/m(\ell\nu J) > 0.3(0.4)$ for VBF (ggF) selection
  - $p_{\mathrm{T}}(J)/m(\ell\nu J) > 0.3(0.4)$ for VBF (ggF) selection.

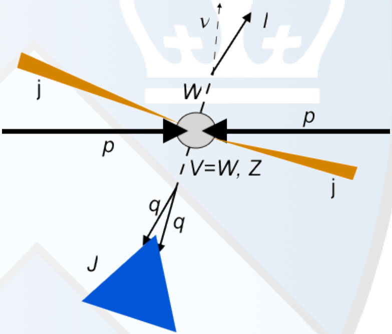

Signal Regions (SR) and Control Regions (CR)

- Use large-R jet substructure (D_2) and mass (around W/Z peaks) to define SRs
- Define CRs kinematically close to SRs

High Purity (HP) Selection

- SR
  - No b-jets (outside J)
  - Pass both 50 % eff. working points (w.p.) of boson tagger (mass, D_2)
- W+jets CR: same as SR, except:
  - Fail mass 80 % eff. w.p.
- $t\bar{t}$ CR: same as SR, except:
  - ≥ 1 $b-$jet (outside J)

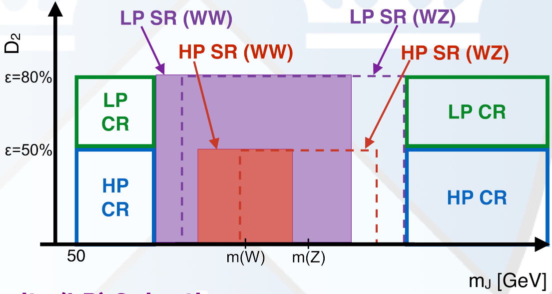

Low Purity (LP) Selection

- SR
  - No $b-$jets (outside J)
  - Fail *at least one* 50 % eff. w.p.
  - Pass *both* 80 % eff. w.p.
- $W+$ jets CR
  - Fail mass 80 % eff. w.p.
  - Fail (pass) D_2 50 % (80 %) eff. w.p.
- $t\bar{t}$ CR: same as SR, except
  - ≥ 1 $b-$jet (outside J)

Signal Region Characteristics

- Signal efficiency plateau $\sim 30-35\,\%$ for ggF selection, $\sim 12\,\%$ for VBF selection
- Look for bump in $m(WV)$ distribution. HP SR offers best discrimination.
- Inclusion of LP SR offers $\sim$ $50\,\%$ increase in signal efficiency (albeit with larger backgrounds)

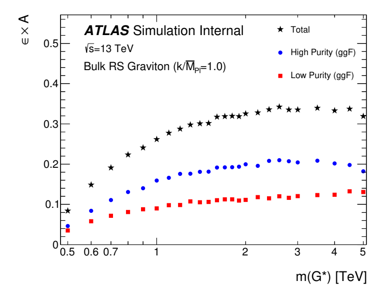

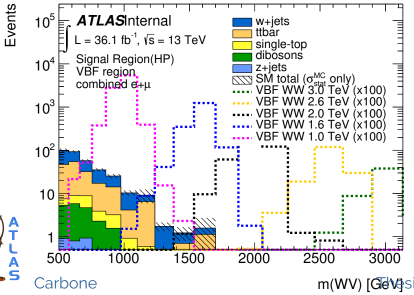

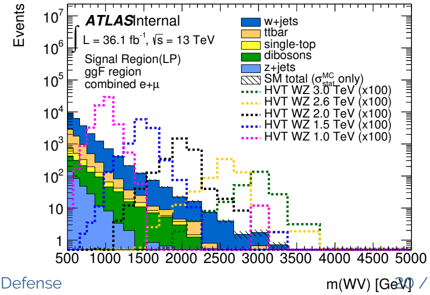

Systematic Uncertainties

- Systematic uncertainties included as nuisance parameters in statistical fit
- "Up"/"down" histograms calculated for sig./bkg. MC by varying systematic uncertainties by $\pm 1\sigma$

Experimental Uncertainties

- Related to reconstructed physics objects affecting bkg. and sig. shape or normalizations
- General: luminosity (3.2 %), pile-up reweighting (match simulated $\langle\mu\rangle$ to that observed in data)
- Leptons: small impact (most $< 1\,\%$) – reconstruction and identification eff., isolation eff., momentum scale and resolution, trigger eff.
- Small-R jets: largest impact from jet energy scale (JES) and resolution ($\sim 1-6\,\%$), b-tagging eff.
  - JES - calibration scheme to correct for non-compensating nature of calorimeters (hadrons lower detector response w.r.t EM objects)
- Large-R jets:
  - scale of p_{T}, m, D_2 ($\sim 2-5\,\%$)
  - resolution of p_{T} (2 % abs. - smear resolution), m (20 % rel.), D_2 (15 % rel.). Relative uncertainties applied such that nom. resolution is increased by specified percentage

Systematic Uncertainties

Background Uncertainties

- Normalizations: Gaussian constraint to account for SM measurement
  - Z+jets/Single-t: 11 % width
  - SM diboson: 30 % width (additional 20 % accounts for factorization/renormalization scales)
- W+jets: shape uncertainties accounting for factorization/renormalization scale, PDF choice (parton distributions), α_S (strong coupling), CKKW matching scale (combine matrix element and showering calculations without doubling counting), resummation scale
- $t\bar{t}$: shape uncertainties accounting for factorization/renormalization scale, MC generator, parton showering

Signal Uncertainties

- Initial State/Final State Radiation: approximately 4 % for most signal models (incoming or outgoing particles emitting photons/gluons unrelated to hard-scatter interaction)
- Choice of PDF: approximately $0.5 - 2\,\%$

Fitting Strategy

$$L(\mu,\theta) = \prod_{j\in\{\text{SRs, CRs}\}} \prod_{i\in\{\text{bins}\}} P(N_{ij}|\mu s_{ij} + B_{ij}) \prod_{l\in\{\text{NPs}\}} \text{Nuis}(\theta_l)$$

Simultaneous Maximum-Likelihood (ML) Fit

- Use binned histogram of invariant mass distribution $m(\ell\nu J)$ as discriminant
- $L(\mu,\theta)$: product of Poisson distributions for each selection region/bin (N_{ij}:# obs. events, s_{ij}:# sig. events, B_{ij}:# bkg. events)
- Signal strength (μ) parameterizes signal production: $\mu = 1$ nominal sig. hyp., $\mu = 0$ bkg-only hyp.
- SRs and CRs fit simultaneously with bkg.-only hyp ($\mu = 0$)
  - E.g. Fit for WW-channel with "ggF selection" includes:
    WW HP SR (ggF), WW LP SR (ggF),
    W+jets HP CR (ggF), W+jets LP CR (ggF),
    $t\bar{t}$ HP CR (ggF), $t\bar{t}$ LP CR (ggF)
- $B_{ij} = \mu_{t\bar{t}} b_{ij}^{t\bar{t}} + \mu_{W+\text{jets}} b_{ij}^{W+\text{jets}} + b_{ij}^{\text{other}}$
  Normalizations of W+jets and $t\bar{t}$ bkgs free to float, extracted from fit
- Systematic uncertainties included as constrained nuisance parameters
- Four fits: WW/WZ channels separately (large overalp), ggF/VBF selection separately

Post-fit Mass Distributions (Control Regions)

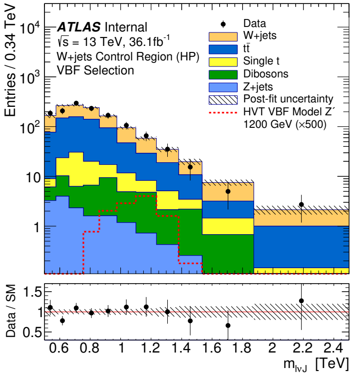

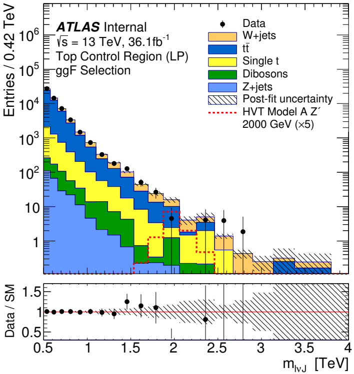

- After ML bkg.-only fit to data, total event yields in CRs consistent with SM bkg. prediction within uncertainties
- Normalization factors for W+jets and $t\bar{t}$ bkgs extracted: range from $0.95 - 1.03$ ($0.85 - 1.2$) for ggF (VBF) selection fits
- Eight total CRs (W+jets, $t\bar{t}$ for HP/LP and ggF/VBF)

Post-fit Mass Distributions (Signal Regions - VBF)

- No significant excesses above the SM prediction are observed
- Total event yields in all SRs consistent with SM background prediction within uncertainties
- *WW*(*WZ*)-channel in left (right) column. HP (LP) SR in top (bottom) row

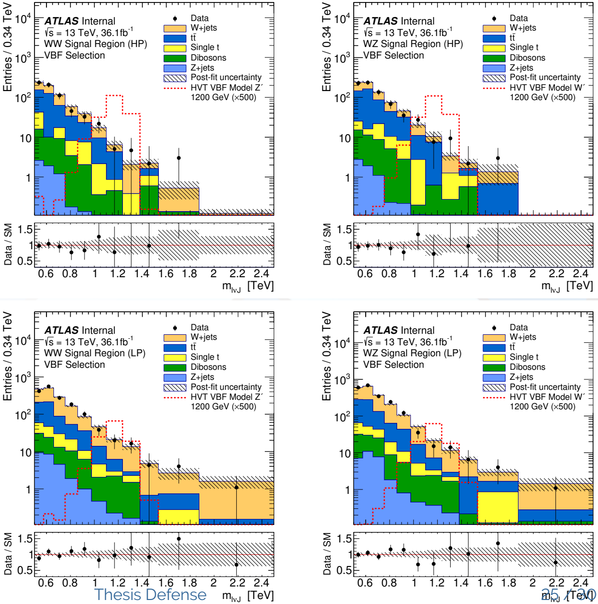

Post-fit Mass Distributions (Signal Regions - ggF)

- No significant excesses above the SM prediction are observed
- *WW*(*WZ*)-channel in left (right) column. HP (LP) SR in top (bottom) row

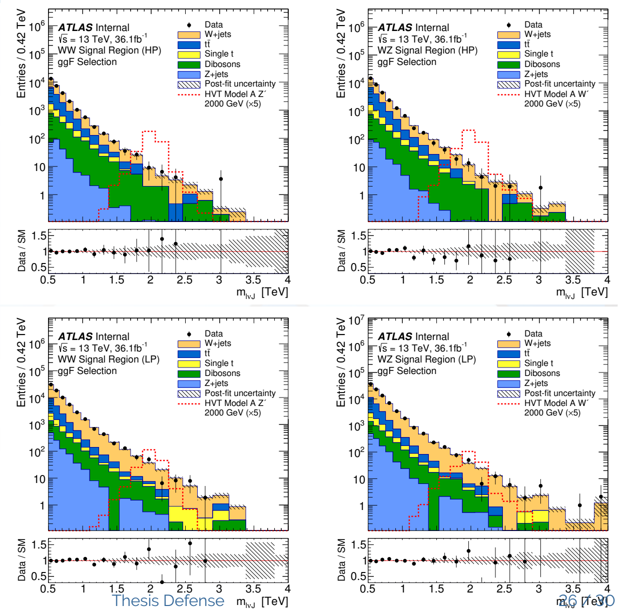

Upper Limits - RS G^*, HVT W'/Z' (ggF Selection)

- To set upper limits, fits performed again with s+b hyp., scanning μ to find $CL_s = 0.05$
- Expected upper limits with $\pm 1\sigma$, $\pm 2\sigma$ uncertainty bands overlaid with observed upper limits

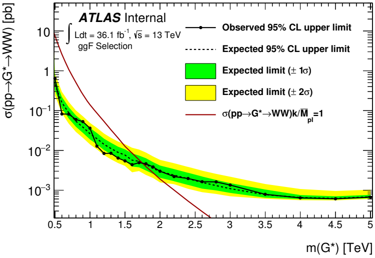

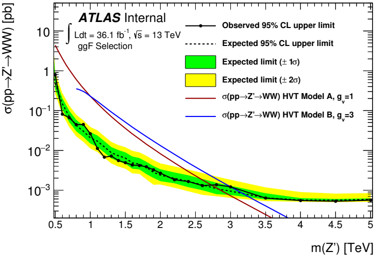

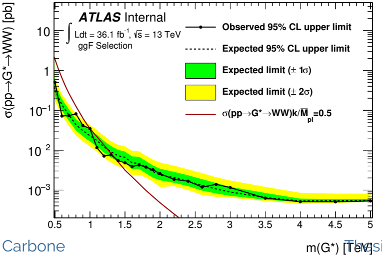

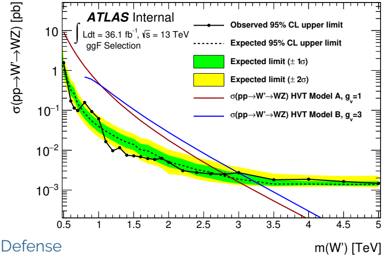

Upper Limits -HVT W'/Z', Heavy Higgs (VBF Selection)

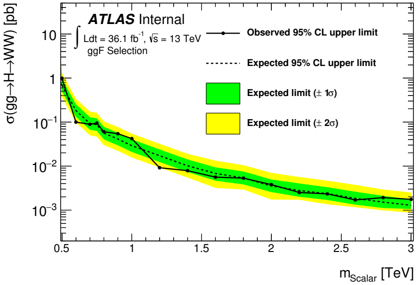

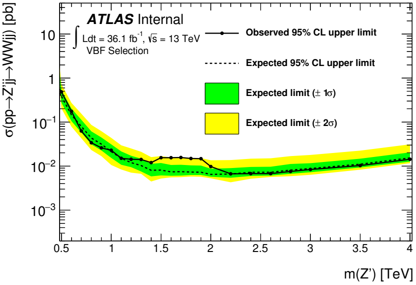

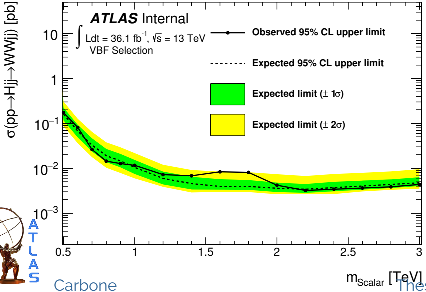

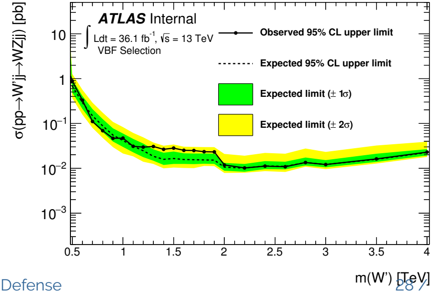

Excluded Resonance Masses

Excluded Masses (95 % CL)

- For models with predicted cross sections overlaid, masses below intersection of prediction and obs. upper limit are excluded at 95 % CL:

Signal Model	**Excluded Masses at 95 % CL**	
WZ Selection	Expected [GeV]	Observed [GeV]
HVT W'		
Model A ($g_V = 1$)	< 2880	< 2800
Model B ($g_V = 3$)	< 3220	< 2990
WW Selection	Expected [GeV]	Observed [GeV]
HVT Z'		
Model A ($g_V = 1$)	< 2830	< 2730
Model B ($g_V = 3$)	< 3170	< 3000
RS G^*		
$\kappa/\overline{M}_{\mathrm{Pl}} = 1.0$	< 1740	< 1750
$\kappa/\overline{M}_{\mathrm{Pl}} = 0.5$	< 1250	< 980 and $1020 - 1350$

Extend Previous Results [1] [2]

- ATLAS result extended by 450 GeV (390 GeV) for W', 380 GeV (400 GeV) for Z', for HVT model-A (model-B)
- Mass range extended by 650 GeV for bulk G^* with $\kappa/\overline{M}_{\mathrm{Pl}} = 1.0$
- First mass exclusion for bulk G^* with $\kappa/\overline{M}_{\mathrm{Pl}} = 0.5$
- ATLAS/CMS results combined multiple final state channels

[1] CMS Collaboration, JHEP 03 (2017) 162. ($2.7\,\mathrm{fb}^{-1}$, $\sqrt{s} = 13$ TeV)
[2] ATLAS Collaboration, JHEP 09 (2016) 173. ($3.2\,\mathrm{fb}^{-1}$, $\sqrt{s} = 13$ TeV)

Conclusions

- Search performed for new resonances
  - Decay to pair of boosted weak bosons (WV, with $V = W/Z$)
  - W decays leptonically, V decays hadronically
  - Consider benchmark signal models
    - Neutral heavy Higgs (spin-0)
    - Heavy vector triplet W'/Z' (spin-1)
    - Randall-Sundrum bulk graviton (spin-2)
- Results consistent with SM background prediction
- Upper limits on cross section set at 95 % CL
  - W'/Z' masses excluded below $2.8 - 3.0$ TeV (depending on model)
  - RS bulk G^* masses excluded below 1.7 TeV ($\kappa/\overline{M}_{\mathrm{Pl}} = 1.0$)
- Diboson resonances remain vital probe of physics BSM, common prediction of many theories
- Going forward, LHC will remain sensitive to rare processes
  - Run II (present-2018): collect up to 150 fb^{-1}
  - Run III (2021-2023): increased $\sqrt{s}$ (14 TeV), increased inst. lumi (2×10^{34}cm^{-2}s^{-1}), total data ~300 fb^{-1}
  - HL-LHC (~ 2026-): increased inst. lumi (~7 times nom. value), total data $\sim$ 3000 fb^{-1}

Backup

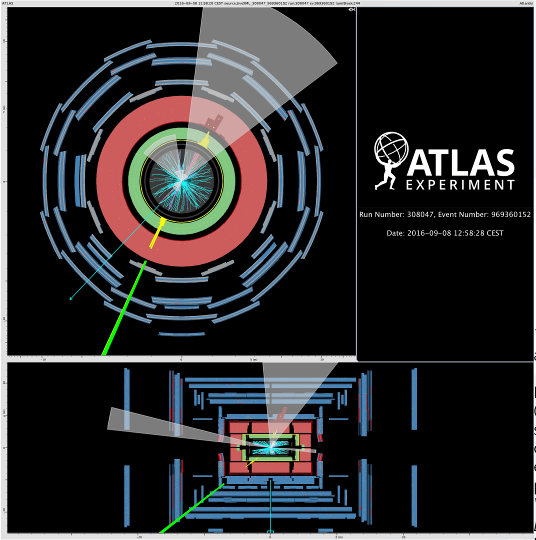

	VBF Candidate
Kinematic Information	
$m(WV \to \ell\nu J)$ [GeV]	2759.33
$E_{\mathrm{T}}^{\mathrm{miss}}$ [GeV]	362.13
p_{T}(lepton) [GeV]	777.14
$p_{\mathrm{T}}(W \to \ell\nu)$ [GeV]	1137.71
$m(J)$ [GeV]	88.80
$D_2^{\beta=1}$	1.632
$m^{\mathrm{VBF}}(j,j)$ [GeV]	811.55
$\Delta\eta^{\mathrm{VBF}}(j,j)$	5.680
Boson Tagger†	
Pass $D_2^{\beta=1}$ 50 % (80 %)	No (Yes)
Pass W mass 50 % (80 %)	Yes (Yes)
Pass Z mass 50 % (80 %)	Yes (Yes)

† The SmoothedWZTagger 50 % and 80 % working points are used to classify the High-Purity and Low-Purity regions.

Event display for the event with the largest $m(WV)$ (2.76 TeV) passing VBF event selection. The top panel shows the event projection in the $R-\phi$ plane looking down the beamline, and the bottom panel shows the event projection in the $R-z$ plane. In the bottom panel, the two forward VBF jets are clearly visible. The $W \to \ell\nu$ decay is shown by the electron (green line) and $E_{\mathrm{T}}^{\mathrm{miss}}$ (blue arrow) and is nearly back to back with the hadronically decaying boson which is reconstructed as a central large-R jet (white cone).

Trigger

Event Triggers

- Lowest un-prescaled single *e* triggers
- HLT_e26_lhtight_nod0_ivarloose: $E_{\mathrm{T}} > 26$ GeV(at HLT), tight LH ID, no transverse impact parameter requirements, and loose variable cone Iso. Higher E_{T} triggers have no Iso. and looser Id. requirements
- μ triggers have $\sim 70\,\%$ eff (limited coverage of MS) $\Rightarrow$ use $E_{\mathrm{T}}^{\mathrm{miss}}$ trigger instead
- At trigger level, $E_{\mathrm{T}}^{\mathrm{miss}}$ calculated only using calorimeter energy, ignoring contributions in MS. $E_{\mathrm{T}}^{\mathrm{miss}}$ at trigger level corresponds to $E_{\mathrm{T}}(W \to \mu\nu)$ at reconstruction level
- $> 90\,\%$ ($100\,\%$) eff. for *e* (μ) triggers at plateau

Data Period	*e*-channel	μ-channel
2015	HLT_e24_lhmedium_L1EM20 OR HLT_e60_lhmedium OR HLT_e120_lhloose	HLT_xe70
2016a (run < 302919) ($\mathcal{L}_{\mathrm{inst.}} < 1.0 \times 10^{34}\mathrm{cm}^{-2}\mathrm{s}^{-1}$)	HLT_e26_lhtight_nod0_ivarloose OR HLT_e60_lhmedium_nod0 OR HLT_e140_lhloose_nod0	HLT_xe90_mht_L1XE50
2016b (run ≥ 302919) ($\mathcal{L}_{\mathrm{inst.}} < 1.4 \times 10^{34}\mathrm{cm}^{-2}\mathrm{s}^{-1}$)	same as 2016a	HLT_xe110_mht_L1XE50

Event Selection

Selection: HP (LP)		SR	W CR	$t\bar{t}$ CR
Production Category	VBF	$m^{\mathrm{VBF}}(j,j) > 770$ GeV and $\lvert\Delta\eta^{\mathrm{VBF}}(j,j)\rvert > 4.7$		
	ggF	Fail VBF selection		
$W \rightarrow \ell\nu$	Signal leptons	1		
	Veto leptons	0		
	$E_{\mathrm{T}}^{\mathrm{miss}}$ [GeV]	> 100		
	$E_{\mathrm{T}}^{\mathrm{miss}}/p_{\mathrm{T}}(e\nu)$	> 0.2		
	$p_{\mathrm{T}}(\ell\nu)$ [GeV]	> 200		
$W/Z \rightarrow J$	Large-R jets	≥ 1		
	$D_2^{(\beta=1)}$ 50 % WP	pass (fail†)	pass (fail)	pass (fail†)
	$D_2^{(\beta=1)}$ 80 % WP	— (pass)	— (pass)	— (pass)
	W/Z mass 50 % WP	pass (fail†)	— (—)	pass (fail†)
	W/Z mass 80 % WP	— (pass)	fail (fail)	— (pass)
Topology Cuts	$p_{\mathrm{T}}(\ell\nu)/m(WV)$	> 0.3 for VBF and > 0.4 for ggF selection		
	$p_{\mathrm{T}}(J)/m(WV)$	> 0.3 for VBF and > 0.4 for ggF selection		
Num. b-jets	$\Delta R(J,b) > 1.0$	0		≥ 1

Summary of selection criteria used to define the SR, W+jets CR and $t\bar{t}$ CR, for HP and LP selections. LP selections are listed in parentheses. Events are categorized according to their production mechanism where VBF selection is prioritized.

† For LP SR and LP $t\bar{t}$ CR, the large-R jet can fail either the 50 % efficiency $D_2^{\beta=1}$ working point or the 50 % efficiency mass window working point.

Signal Region

Main bkg. composition in SRs

- HP SR for VBF (ggF) selection:
  - W+jets: 50 % (60 %)
  - $t\bar{t}$: 45 % (30 %)
- LP SR for VBF (ggF) selection:
  - W+jets: 70 % (75 %)
  - $t\bar{t}$: 25 % (20 %)

Selection Priority

- Prioritize VBF selection
- Small signal leak for ggF (qqF) production samples into VBF selection SR (< 1 %)

Fit Regions for Each Interpretation

Model	ggF Selection (SRs & CRs)		VBF Selection (SRs & CRs)	
	WW	WZ	WW	WZ
Scalar Heavy Higgs				
ggF prod.	✓			
VBF prod.			✓	
HVT $\mathbf{Z'}$				
qqF prod.	✓			
VBF prod.			✓	
HVT $\mathbf{W'}$				
qqF prod.		✓		
VBF prod.				✓
RS $\mathbf{G^*}$	✓			

Summary of selection regions included in maximum likelihood fit for each benchmark signal model. For each selection, all of corresponding HP and LP SR/CR are included. For example, in fit corresponding to ggF selection, WW channel, the following regions are included in the simultaneous fit: HP SR (WW), LP SR (WW), HP W+jets CR, LP W+jets CR, HP $t\bar{t}$ CR and LP $t\bar{t}$ CR, with all regions passing the ggF selection.

Event Yields (VBF Selection)

Expected and observed event yields in the signal regions and control regions for the VBF WW and WZ selections. Yields and uncertainties are evaluated after a background-only fit to the data in all regions indicated above. The uncertainty on the total background estimate can be smaller than the quadratic sum of the individual background contributions due to anti-correlations between the estimates of different background sources.

VBF WW	High Purity			Low Purity		
Selection	SR	W+jets CR	Top CR	SR	W+jets CR	Top CR
W+jets	71 ± 15	183 ± 26	18 ± 4	268 ± 31	294 ± 35	55 ± 11
$t\bar{t}$	84 ± 16	179 ± 22	346 ± 19	115 ± 24	225 ± 30	500 ± 27
Single-t	13 ± 3	24 ± 6	30 ± 5	23 ± 5	31 ± 6	47 ± 9
SM Diboson	9.8 ± 3.4	13 ± 4	3.3 ± 1.1	17 ± 6	16 ± 5	6.7 ± 3.2
Z+jets	1.6 ± 0.5	4.5 ± 0.9	0.5 ± 0.3	6.7 ± 2.1	8.7 ± 2.1	2.0 ± 0.7
Total Background	178 ± 12	403 ± 19	398 ± 18	431 ± 20	573 ± 23	611 ± 23
Observed	176	402	398	436	567	613

VBF WZ	High Purity			Low Purity		
Selection	SR	W+jets CR	Top CR	SR	W+jets CR	Top CR
W+jets	75 ± 17	187 ± 27	18 ± 5	323 ± 42	302 ± 41	58 ± 12
$t\bar{t}$	106 ± 24	175 ± 45	346 ± 36	161 ± 49	224 ± 56	496 ± 52
Single-t	12 ± 6	24 ± 10	31 ± 10	26 ± 11	30 ± 9	47 ± 19
SM Diboson	10 ± 5	11 ± 5	2.7 ± 1.1	22 ± 10	14 ± 5	5.9 ± 4.1
Z+jets	1.6 ± 1.5	4.6 ± 2.3	0.4 ± 0.2	7.8 ± 6.0	8.4 ± 3.9	1.9 ± 1.2
Total Background	205 ± 28	402 ± 52	398 ± 41	540 ± 49	578 ± 47	609 ± 66
Observed	201	402	398	550	567	613

Event Yields (ggF Selection)

Expected and observed event yields in the signal regions and control regions for the ggF *WW* and *WZ* selections. Yields and uncertainties are evaluated after a background-only fit to the data in all regions indicated above. The uncertainty on the total background estimate can be smaller than the quadratic sum of the individual background contributions due to anti-correlations between the estimates of different background sources.

ggF *WW*	High Purity			Low Purity		
Selection	SR	*W*+jets CR	Top CR	SR	*W*+jets CR	Top CR
W+jets	3116 ± 165	6848 ± 206	540 ± 60	10790 ± 251	10972 ± 255	1424 ± 167
$t\bar{t}$	2043 ± 142	2920 ± 180	6883 ± 138	2648 ± 187	3790 ± 222	8738 ± 235
Single-*t*	374 ± 44	487 ± 57	704 ± 84	493 ± 56	553 ± 64	819 ± 97
SM Diboson	353 ± 94	167 ± 45	51 ± 14	431 ± 118	201 ± 55	70 ± 20
Z+jets	49 ± 6	143 ± 17	15 ± 3	205 ± 25	215 ± 27	54 ± 9
Total Background	5935 ± 70	10565 ± 96	8192 ± 87	14566 ± 120	15730 ± 124	11105 ± 104
Observed	5885	10619	8178	14566	15707	11133

ggF *WZ*	High Purity			Low Purity		
Selection	SR	*W*+jets CR	Top CR	SR	*W*+jets CR	Top CR
W+jets	3679 ± 173	6958 ± 191	556 ± 61	13356 ± 299	11091 ± 247	1496 ± 173
$t\bar{t}$	2283 ± 146	2812 ± 167	6842 ± 141	3447 ± 233	3681 ± 218	8611 ± 241
Single-*t*	410 ± 50	485 ± 57	749 ± 90	655 ± 75	556 ± 65	854 ± 102
SM Diboson	356 ± 98	162 ± 44	51 ± 14	498 ± 138	193 ± 53	71 ± 21
Z+jets	56 ± 7	148 ± 18	15 ± 3	244 ± 31	212 ± 26	55 ± 9
Total Background	6784 ± 76	10564 ± 96	8211 ± 88	18201 ± 136	15733 ± 124	11087 ± 104
Observed	6751	10619	8178	18188	15707	11133

Local p-values

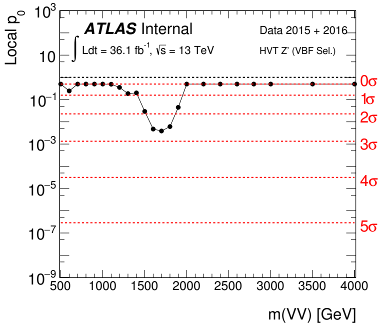

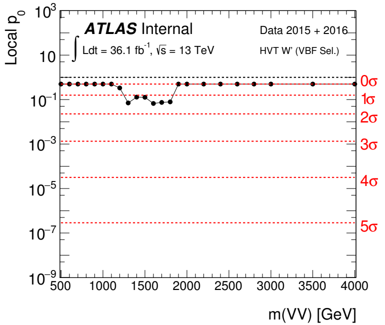

Local p-value for the tested HVT W' and HVT Z' signal models. The mass region greater than 1.5 TeV is covered by two bins in the final discriminant.

QCD Estimation - Contamination

- Although lepton Iso./ID w.p. have large rejection ratios, QCD multi-jet cross section is very large. May contaminate CRs/SRs as reconstructed fake leptons.
- Fake electrons mostly from heavy quark decays, photon conversions, and hadrons faking electrons. Non-prompt muons from b/c hadron decays are main source of fake muons
- Multi-jet bkg. steeply falling with $E_{\mathrm{T}}^{\mathrm{miss}}$ $\Rightarrow$ require $E_{\mathrm{T}}^{\mathrm{miss}} > 100$ GeV (contamination to less than 1 % in 2016)
- Discrepancy in e-channel between data/MC for high-$p_{\mathrm{T}}(e)$ in W+jets CR.
- High-p_{T} events in e-channel with small $E_{\mathrm{T}}^{\mathrm{miss}}$ (with respect to the $p_{\mathrm{T}}(e)$) were most likely multi-jet events faking an electron.
- Relatively low stats in the high-p_{T} region amplified effect of previously estimated small QCD contamination
- Solution: implement new mutli-jet cut, requiring $E_{\mathrm{T}}^{\mathrm{miss}}/p_{\mathrm{T}}(W \to e\nu) > 0.2$

QCD Estimation - Multijet Cut

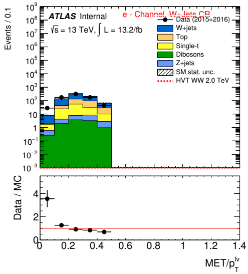

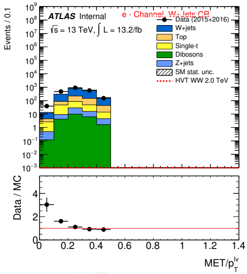

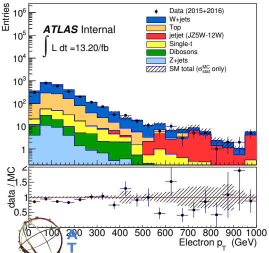

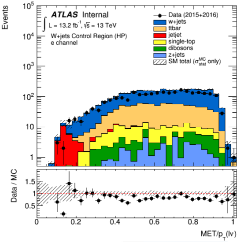

- (Top row) $E_{\mathrm{T}}^{\mathrm{miss}}/p_{\mathrm{T}}(W)$ in W+jets CR with inverted $E_{\mathrm{T}}^{\mathrm{miss}}$ cut. Multijet events have characteristically low $E_{\mathrm{T}}^{\mathrm{miss}}$, largest discrepancy seen in exactly this region
- (Bottom row) Dijet MC samples generated to validate hypothesis. (Left) Dijet MC is concentrated in high-$p_{\mathrm{T}}(e)$ region where discrepancy observed. (Right) Shows dijet MC largely contained in region $E_{\mathrm{T}}^{\mathrm{miss}}/p_{\mathrm{T}}(W) < 0.2$

QCD Estimation - Data Driven Fit - I

- Data driven estimation (13.2 fb^{-1}) - CR defined with expected multi-jet enrichment
- Extract a shape template (separately for HP/LP selection) by subtracting MC prediction from data, then use template to fit nominal W+jets CR, estimate contamination
- CR: e fail nominal Iso./ID cuts, μ fail nominal Iso/impact parameter cuts. Leptons must pass "Loose" Iso. w.p. (99 % eff.) and Id. w.p.. No cut on $E_{\mathrm{T}}^{\mathrm{miss}}$. Rest of cuts for either the SR or W+jets CR.
- Shape extracted from $E_{\mathrm{T}}^{\mathrm{miss}}$ distribution, only fit above 50 GeV (triggers still affecting low $E_{\mathrm{T}}^{\mathrm{miss}}$ region)
- Normalization of the MC bkg allowed to float within statistical uncertainties in fit
- For e-channel, the contamination for $E_{\mathrm{T}}^{\mathrm{miss}} > 100$ GeV (selection used in analysis) consistent with zero events.
- For μ-channel, the multi-jet contamination in multijet CR is already negligible

QCD Estimation - Data Driven Fit - II

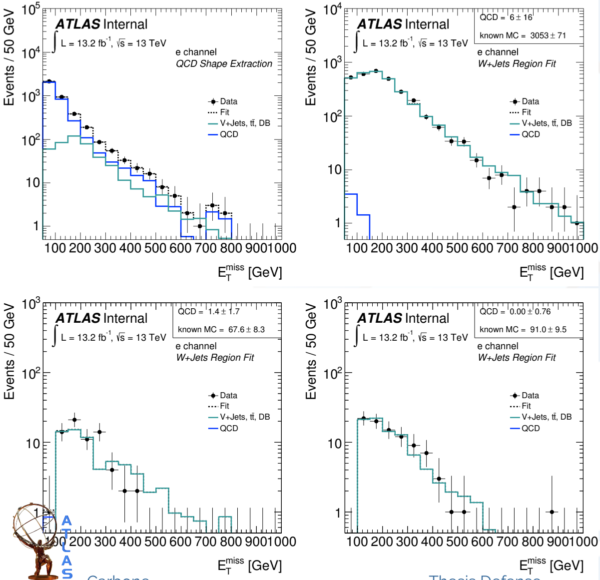

- (Top Row) (Left) QCD shape extraction from QCD-enriched CR (Right) Results of data-driven template fit to nominal W+jets CR (e-channel, HP). Results consistent with no events for $E_{\mathrm{T}}^{\mathrm{miss}} > 100$ GeV.
- (Bottom Row) Results of the fit restricted to events with large electron momentum ($p_{\mathrm{T}}(e) > 400$ GeV), also consistent with zero events. (left - HP, right - LP)

Neutrino p_z - I

- Along beam axis, $\hat{z}$, an unknown fraction of energy from event escapes $\Rightarrow$ restricts ability to constrain missing energy to transverse $\hat{x} - \hat{y}$ plane
- For this analysis ($WV \to l\nu J$), neutrino escapes detector leaving virtually no energy deposit; thus, missing energy in the transverse plane, $E_{\mathrm{T}}^{\mathrm{miss}}$, attributed to transverse momentum of neutrino, $p_{\mathrm{T},\nu}$.
- Invariant mass of WV system is given below:

$$m(WV)^2 = (E_J + E_l + E_\nu)^2 - \left(\vec{p}_J + \vec{p}_l + \vec{p}_\nu\right)^2$$

- Since only transverse momentum of neutrino is known, however, the transverse mass, m_{T}, must be used:

$$m_{\mathrm{T}}(WV)^2 = \left(E_{\mathrm{T},J} + E_{\mathrm{T},l} + E_{\mathrm{T},\nu}\right)^2 - \left(\vec{p}_{\mathrm{T},J} + \vec{p}_{\mathrm{T},l} + \vec{p}_{\mathrm{T},\nu}\right)^2$$

- $m_{\mathrm{T}}(WV)$ depends on angle between daughter particles, worse resolution than $m(WV)$ (better signal to background ratio)
- Choose to reconstruct $\hat{z}$ component of neutrino momentum vector, $p_{z,\nu}$, with constraint of W boson mass ($m(W) = 80.385$ GeV)
- Using energy-momentum 4-vectors, $p^\mu = (E, \vec{p})$, for W boson, lepton, and neutrino, a quadratic expression for $p_{z,\nu}$ in terms of m_W, $\vec{p}_l$, and $p_{\mathrm{T},\nu}$ can be derived

Neutrino p_z - II

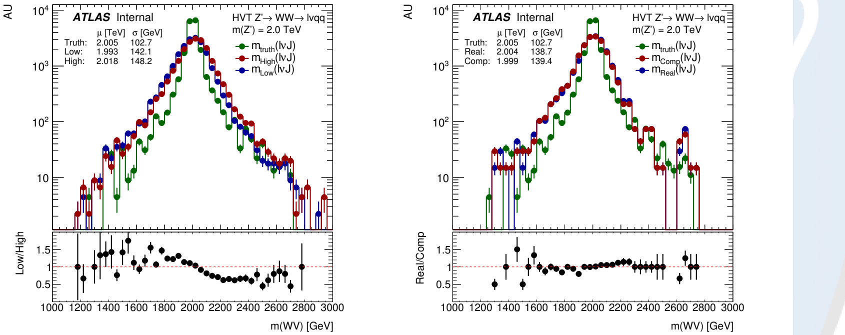

- HVT Z' benchmark signal at $m = 2.0\,\text{TeV}$ used.
- There can be up to two solutions for $p_{z,\nu}$, which are handled as follows:
  - If a solution is complex, remove the imaginary part
  - If two unique solutions exist, compare the magnitudes and keep the smallest one
- Effect of these choices are minimal

Standard Model

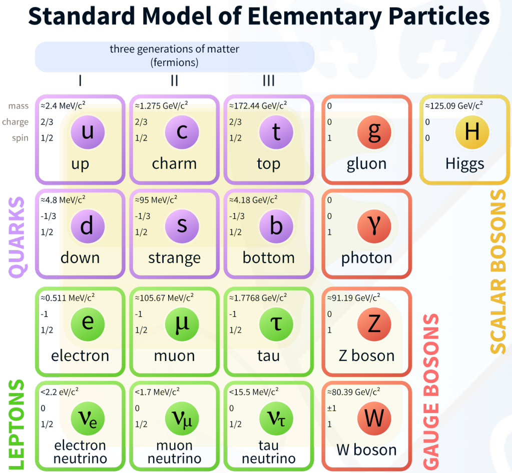

- Particles have intrinsic property "spin", form of angular momentum
- Fermions (spin-1/2)
  - Leptons: interact with EM, weak forces
  - Quarks: make up hadrons (2-3 quarks), interact with EM, weak, strong forces
- Gauge bosons (spin-1) mediate forces
- Higgs boson(spin-0) - generates mass for massive fundamental particles

- Standard Model (SM) describes physics well up to TeV-scale, but incomplete (dark matter, neutrino masses, matter-antimatter asymmetry, etc.)

Local Gauge Symmetry [$U(1)$]

$$
\begin{aligned}
\mathcal{L} &= \bar{\psi}(\gamma^{\mu}\partial_{\mu} - m)\psi \\
\psi(x) &\rightarrow \psi'(x) = e^{i\alpha(x)}\psi(x) \\
\partial_{\mu} &\rightarrow D_{\mu} = \partial_{\mu} - ieA_{\mu} \\
A_{\mu}(x) &\rightarrow A'_{\mu}(x) = A_{\mu}(x) + \frac{1}{e}\partial_{\mu}\alpha(x) \\
\mathcal{L}' &= \bar{\psi}e^{-i\alpha}\left[\gamma^{\mu}\partial_{\mu} - ie\gamma^{\mu}\left(A_{\mu} + \frac{1}{e}\partial_{\mu}\alpha\right) - m\right]e^{i\alpha}\psi \\
&= \bar{\psi}(e^{-i\alpha+i\alpha})\left[i\gamma^{\mu}(\partial_{\mu}\alpha) + \gamma^{\mu}\partial_{\mu} - ie\gamma^{\mu}\left(A_{\mu} + \frac{1}{e}(\partial_{\mu}\alpha)\right) - m\right]\psi \\
&= \mathcal{L}
\end{aligned}
$$

- Symmetry of field described by Lie Algebra of $U(1)$ with one generator (i.e. α)
- $\alpha(x)$ depends on coordinates $\rightarrow$ local symmetry
- Gauge field, A_{μ}, preserves local gauge invariance (need one per generator)
- Gauge field introduces an interaction term with original fields: $-ie\bar{\psi}\gamma^{\mu}A_{\mu}\psi$
- Can add kinetic term for propagation of gauge field: $F^{\mu\nu} \equiv \partial^{\mu}A^{\nu} - \partial^{\nu}A^{\mu}$
- Adding mass terms for gauge fields (e.g. Proca equation) violates gauge invariance (need Higgs mechanism)

Planck Scale

- Scale at which predictions of SM expected to break down
- $m_{\text{Planck}} = \sqrt{\hbar c/G} = 1.22 \times 10^{19}$ GeV
  - Dimensional analysis to define quantity with units of mass using fundamental constants
- $M_{\text{Planck}} = m_{\text{Planck}}/\sqrt{8\pi}$
  - Reduced Planck mass
  - Used to make equations look nicer

Extended Higgs Sector

- Can introduce mechanisms for CP violation to explain matter-antimatter imbalance, offer Dark Matter candidate, and explain neutrino masses without right-handed neutrino
- Simplest extension is 2HDM: extra complex scalar doublet
- Usually impose $\mathbb{Z}_2$ symmetry to exclude tree-level FCNC $(\Phi_1 \to \Phi_1, \Phi_2 \to -\Phi_2)$
- $V = m_{11}^2 \Phi_1^\dagger \Phi_1 + m_{22}^2 \Phi_2^\dagger \Phi_2 - (m_{12}^2 \Phi_1^\dagger \Phi_2 + h.c.) + \frac{\lambda_1}{2}(\Phi_1^\dagger \Phi_1)^2 + \frac{\lambda_2}{2}(\Phi_2^\dagger \Phi_2)^2 + \lambda_3 \Phi_1^\dagger \Phi_1 \Phi_2^\dagger \Phi_2 + \lambda_4 \Phi_1^\dagger \Phi_2 \Phi_2^\dagger \Phi_1 + (\frac{\lambda_5}{2}(\Phi_1^\dagger \Phi_2)^2 + h.c.)$
- V is hermitian, so m_{12}^2, λ_5 can be complex, rest of parameters must be real
- Choose vev's real, define $\tan\beta = v_2/v_1$
- For CP-conserving theory: CP-even neutral scalars: h, H, CP-odd neutral scalar: A, charged scalar: $H^\pm$
- Independent parameters: $m_h, m_H, m_A, m_{H^\pm}, m_{12}^2$ and α (describes angle of CP-even mass mixing)

Extended Higgs - Singlet

- $V = \frac{m^2}{2}H^\dagger H + \frac{\lambda}{4}(H^\dagger H)^2 + \frac{\delta_1}{2}H^\dagger HS + \frac{\delta}{2}H^\dagger HS^2 + \left(\frac{\delta_1 m^2}{2\lambda}\right)S + \frac{\kappa_2}{2}S^2 + \frac{\kappa_3}{3}S^3 + \frac{\kappa_4}{4}S^4$
- Singlet field, S, has no vev, H, m, λ are normal SM Higgs doublet parameters
- δ_1 controls mixing between S and SM h
  - If no mixing, $m(S)$ determined by κ_2, δ_2
  - In general, can mix, implies S can couple to all fields SM h couples to
- If impose $\mathbb{Z}_2$ symmetry ($\delta_1 = \kappa_3 = 0$), no vertices with odd number of S
  - Scalar singlet is stable
  - Can be candidate for DM
  - Only interacts with proton through t-channel exchange of SM higgs with quarks or gluons (through quark loop)

Composite Higgs

- Explain EWSB without a fundamental complex scalar doublet
- New strongly interacting sector, with extended gauge symmetry
- Careful choice of extended symmetry, spontaneous symmetry breaking in new strongly interacting sector at scale $\Lambda_{\text{comp}} << \Lambda_{\text{Planck}}$
  - In HVT Model-B: $SO(5) \rightarrow SO(4)$
  - Addresses hierarchy problem
  - Produce Goldstone boson which transforms as SM Higgs doublet
  - Unbroken symmetry group corresponds to SM $SU(2) \times U(1)$ EW symmetry
- Larger global symmetry is additionally explicitly broken (e.g. with Yukawa mass terms)
  - Explicit breaking of the larger symmetry causes goldstone boson (i.e. composite Higgs) to not be exactly massless
  - The approximate symmetry, however, keeps mass low (addresses naturalness)
- New gauge bosons predicted corresponding to the additional symmetries of the the strongly interacting sector

Extended Gauge Group

- In general, any enlarged symmetry group which is spontaneously broken into the SM $SU(2)_L \times U(1)_Y$
- HVT Model-A
  - Larger symmetry: $SU(2)_1 \times SU(2)_2 \times U(1)_Y \to SU(2)_L \times U(1)_Y$
  - SM fermions charged under $SU(2)_1, U(1)_Y$ with usual quantum numbers
  - SM Higgs doublet $(2,1)_{1/2}$ in extended group
  - Additional scalar field, Φ, which is a bi-doublet, $(2,2)_0$
  - $\langle\Phi\rangle = \mathrm{diag}(f, f)$ breaks symmetry to SM subgroup
- GUT motivated by $\Lambda_{\mathrm{GUT}} \sim 10^{16}$ GeV, near convergence of 3 gauge couplings
  - Electric charge quantization
  - $SU(5)$ smallest group, $SO(10)$ predicts no extra fermions and each generation transforms in one irreducible multiplet
- Gauge bosons predicted corresponding to generators of extended symmetries
- Series of symmetry breaking scales reduce larger symmetry to SM gauge group
- Gauge bosons of broken symmetries acquire mass near symmetry breaking scales

Kaluza-Klein Excitation

- In the Kaluza Klein model, a massless scalar $\phi(x^\mu, x^5)$ has quantized motion in the periodic dimension: $p^5 = \frac{n}{R}$
- A Fourier expansion of the field in the fifth dimension yields, $\phi(x^\mu, x^5) = \sum_n \phi^n(x^\mu) e^{inx^5/R}$
- An equation of motion for ϕ in $(3+1)$ dimensions can be given: $\left(\partial_\mu \partial^\mu + \partial_5 \partial^5\right)\phi = 0 \qquad \Rightarrow \partial_\mu \partial^\mu \phi^n(x^\mu) = \frac{n^2}{R^2}\phi^n(x^\mu)$
- This describes an infinite tower of fields $\phi^n(x^\mu)$ with masses $m^2 = \frac{n^2}{R^2}$
- For higher spin fields, the procedure is more complicated but a similar reduction produces a tower of massive KK excitations

Randall-Sundrum Graviton

- $ds^2 = e^{-2kr_c|\phi|}\eta_{\mu\nu}dx^\mu dx^\nu + r_c^2 d\phi^2$
- r_c describes size of extra dimension ϕ
- $kr_c \simeq 12$, hierarchy on TeV brane produced geometrically from warping factors
- Physical mass parameters on TeV-brane have warping factor from higher dimensional values: $m = e^{-kr_c\pi}m_0$
- Propagation of massless graviton in bulk creates tower of Kaluza-Klein excitations
- In bulk RS model, SM fields can propagate and are localized in bulk
  - Fields with lighter masses on TeV-brane, localized closer to Planck-brane (larger warping factor)
  - Higgs field still constrained to TeV brane
  - Can additionally address flavor hierarchy by localizing generations at different distances from TeV-brane
  - Since KK excitation localized near TeV-brane, couples strongest to heavy fields and Higgs field (including W_L/Z_L Goldstone modes by equivalence theorem)

Luminosity

$$\mathcal{L} = \frac{1}{4\pi}\left(N_b n_b f_{\mathrm{rev}}\right)\frac{N_b}{\epsilon_n}\frac{\gamma_r}{\beta^*}F(\theta_c, \sigma_z, \beta^*, \epsilon_n)$$

- N_b: #p/bunch (1.1×10^{11})
- n_b: # bunch (2808)
- f_{rev}: rev. freq. (11.245 kHz)
- ϵ_n: norm. emittance ($\sim 3.75\ \mu$m)
- γ_r: Lorentz factor (6927 at 6.5 TeV)
- β^*: betatron function at interaction point (~ 0.55 m)
- F: geometrical factor (~ 0.7)

$$p[\mathrm{TeV}] = 0.3B[\mathrm{TeV}] \cdot R[\mathrm{km}]$$

- 8.33 T superconducting dipole bending magnets

Measuring Amount of Collected Data

- Experiment with instantaneous luminosity, $\mathcal{L}$ [$\text{cm}^{-2}\text{s}^{-1}$], operated over length of time
- Integrated luminosity [fb^{-1}]: $L = \int \mathcal{L} dt$
- Cross section of interaction measured with: $\text{fb} = 10^{-39}$ cm^2 = 2.6×10^{-12} GeV^{-2}
- For collected data corresponding to an integrated luminosity of 100 fb^{-1}, expect 100 events per fb of cross section for specified process
- For Run-II in ATLAS, roughly 2.5 MB/event, 1kHz event output, avg. inst. luminosity $\sim 5 \times 10^{33}\text{cm}^{-2}\text{s}^{-1} = 5 \times 10^{-6}\text{fb}^{-1}\text{s}^{-1}$
- Data stored per fb^{-1} $\sim \frac{2.5\text{GB}}{s} \times \frac{s}{5\times10^{-6}\text{fb}^{-1}} = \frac{500\text{TB}}{\text{fb}^{-1}}$
- For each analysis, total data much smaller $\rightarrow$ trigger events with relevant topology, store only relevant variables, etc.

ATLAS - Inner Detector (ID)

- Surrounded by 2 T solenoid magnet, measures charged particle transverse momentum: p_{T}
- Insertable B-Layer & Pixel Detector: silicon pixel sensors, impact parameter resolution, vertex ident., short-lived particle ident.
- Semiconductor Tracker: silicon strips provide avg. 4 position measurements at intermediate distances
- Transition Radiation Tracker: gas-filled drift tubes, avg. 36 hits/track, transition radiation can differentiate electrons from hadrons

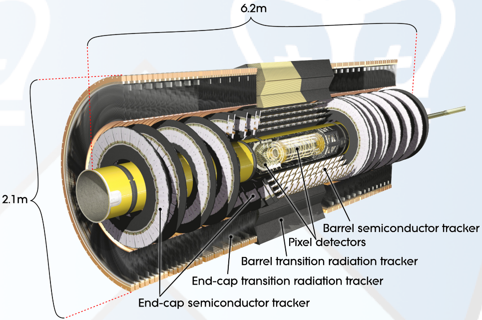

Subsystem	Coverage	Transverse ($R-\phi$) Resolution[μm]	Longitudinal (z) Resolution[μm]	Avg. # Hits
Barrel				
IBL	$\|\eta\| < 2.9$	10	75	1
Pixel	$\|\eta\| < 2.5$	10	115	3
SCT	$\|\eta\| < 1.5$	17	580	4
TRT	$\|\eta\| < 1.0$	130	—	36
Endcap				
Pixel	$2.0 < \|\eta\| < 2.5$	10	115 (R)	3
SCT	$1.3 < \|\eta\| < 2.5$	17	580 (R)	9
TRT	$0.8 < \|\eta\| < 2.0$	130	—	36

ATLAS - Calorimeters

- Alternate dense absorber layers with active medium, fully absorb energy from e, γ, hadrons, measure missing transverse energy $E_{\mathrm{T}}^{\mathrm{miss}}$
- Liquid Argon (LAr) EM ($|\eta| < 3.2$): accordion-shaped lead absorber with active LAr medium, measure EM showers
- LAr Hadronic ($1.5 < |\eta| < 4.9$): copper or tungsten absorbers, active LAr medium
- Tile Hadronic ($|\eta| < 1.7$): steel absorbers with active scintillating plastic tiles

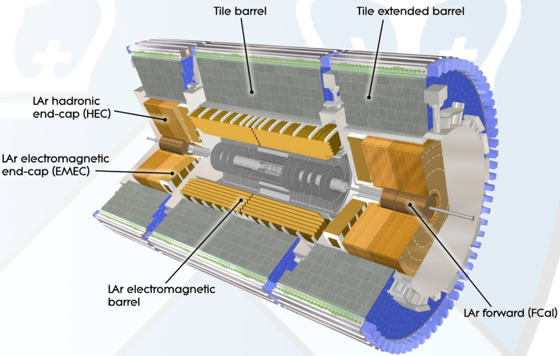

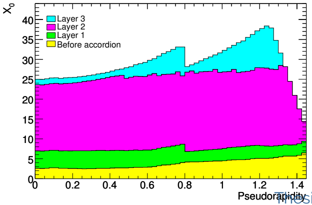

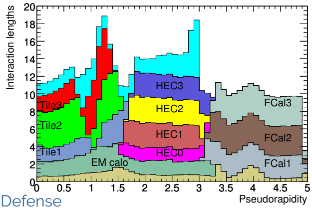

Liquid Argon (LAr) Calorimeter

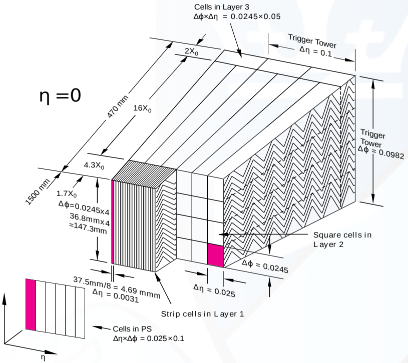

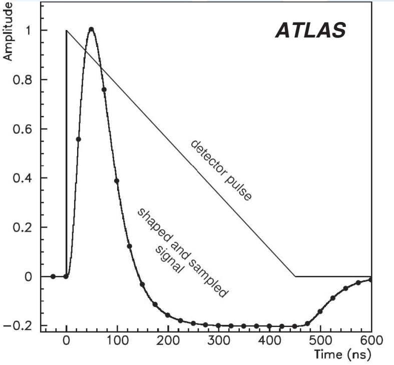

- In EM calorimeter, second layer absorbs bulk of EM radiation, granularity $\Delta\eta \times \Delta\phi = 0.025 \times 0.0245$
- LAr ionized by incident radiation, 450 ns drift time
- Pulse shaped, and sampled every 25 ns (four per pulse)
- Energy and time reconstructed using Optimal Filtering Coefficients (OFCs) calculated during calibration runs, calculated in bins of (25/24) ns

LAr Timing

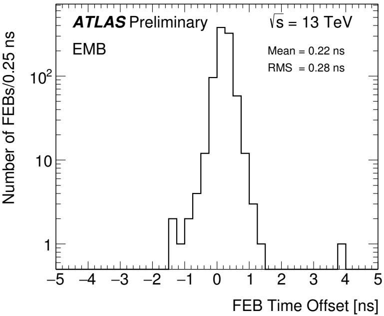

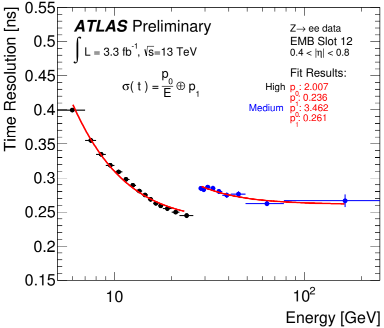

- Online Front-End Board (128 channels) timing, well grouped below 1 ns (0 ns is relativistic particle from center)
- Offline Timing (2015) optimized per channel using $W \rightarrow e\nu$ data
- 7-step calibration, corrects for: time of flight from PV, avg FEB time, avg time per cell, energy dependence, cross talk (position within cell), and cross talk between layers (fractional energy in layer 1 and layer 3)
- Beam spread contributes ~ 200 ps to p_1 (constant term in time resolution)
- If uncorrelated, LAr contribution roughly $100 - 170$ ps in this region

ATLAS - Muon Spectrometer (MS)

- Muons not contained in calorimeters
- Poor resolution of ID tracks for muons in high-p_T regime
- Toroid magnets provide 0.5 T (1.0 T) field in barrel (end-cap)
- Precision tracking chambers: measure p_T and position; monitored drift tubes (barrel), cathode strip chambers (end-cap)
- Trigger chambers: assign correct bunch crossing identification and provide triggering information; resistive plate chambers (barrel), thin gap chambers (end-cap)

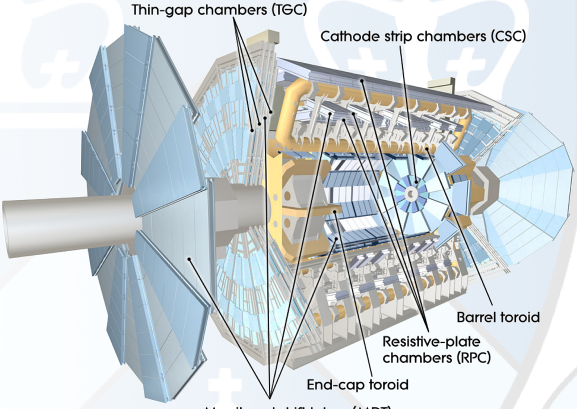

Sub-detector	Coverage	Resolution				Avg. Hits	Type
		z	R	ϕ [mm]	t [ns]		
MDT	$\lvert\eta\rvert < 2.7$	$35\,\mu$m	—	—	—	20	Precision
CSC	$2.0 < \lvert\eta\rvert < 2.7$	—	$40\,\mu$m	5	7	4	Precision
RPC	$\lvert\eta\rvert < 1.1$	10 mm	—	10	1.5	6	Trigger
TGC	$1.1 < \lvert\eta\rvert < 2.4$	—	2-6 mm	3-7	4	9	Trigger

Trigger and Data AcQuisition (TDAQ)

Property	Run-I	Run-II
$\sqrt{s}$ [TeV]	8	13
L_{peak} [10^{33} cm^{-2}s^{-1}]	5.0	13.8
Bunch spacing [ns]	50	25
# bunches	1380	1380-2700
Avg. pile-up	20.7	24.9
Event size [MB]	1.6	2.4
L1 inputs (items)	160 (256)	512 (512)
L1 rate [kHz]	70	100
Total output rate [kHz (GB/s)]	0.6 (0.96)	1.0 (2.4)

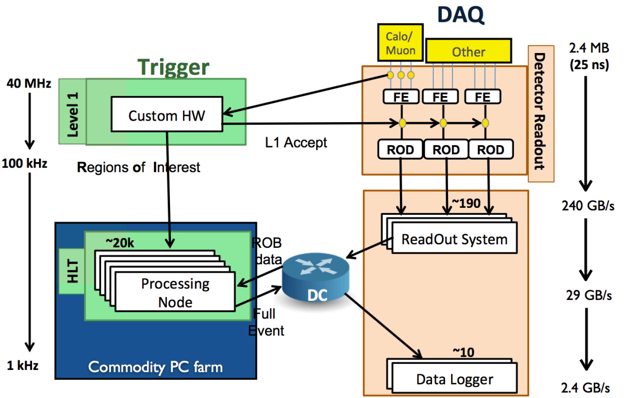

The TDAQ architecture was modified in Run-II by consolidating the Level-2 and Event Filter stages into one High Level Trigger stage. The total event rate increased from 600 Hz in Run-I to 1 kHz in Run-II, in a more challenging environment, with the help of the upgrades and optimizations implemented

Object Reconstruction

Cut	Small-R Jet Definition	
	b-jet Candidate	VBF jet Candidate
Algorithm	Anti-k_{T} $R = 0.4$	
Energy Calibration	EM+JES	
p_{T} [GeV]	> 20	> 30
$\|\eta\|$	< 2.5	< 4.5
Pileup Removal (JVT 92 % efficiency)	if $p_{\mathrm{T}} < 60\,GeV$ && $\|\eta\| < 2.4$	
$b-$tag (85 % eff.)	pass	fail

Cut	Large-R Jet Definition
Algorithm	Anti-k_{T} $R = 1.0$
Grooming	Trimming with $R_{\text{sub-jet}} = 0.2$, $f_{\text{cut}} = 0.05$
Energy Calibration	LCW+JES
p_{T} [GeV]	> 200
$\|\eta\|$	< 2.0
Mass [GeV]	> 50
Boson Tagging	SmoothedWZTagger

Selection	Requirement
Num. VBF candidate jets	≥ 2, select highest $m^{\mathrm{VBF}}(j,j)$ pair
Separate Hemispheres	$\eta(j_1) \cdot \eta(j_2) < 0$
Invariant Mass [GeV]	$m^{\mathrm{VBF}}(j,j) > 770$
Separation	$\|\Delta\eta^{\mathrm{VBF}}(j,j)\| > 4.7$

Cut	Electron Definition	Muon Definition
p_{T} [GeV]	> 27	
$\|\eta\|$	$< 2.47 \notin [1.37, 1.52]$	< 2.5
Identification	TightLH	Medium
Isolation	FixedCutTight	FixedCutTight-TrackOnly
$\|d_0/\sigma(d_0)^{BL}\|$	< 5	< 3
$\|z_0 \sin\theta\|$ [mm]	< 0.5	

Muon Reconstruction

- Combined (CB): The full muon track is reconstructed, starting in the MS and extrapolating towards the ID.
- Segment Tagged (ST): The ID track is extrapolated towards the MS, where it must match at least one MDT/CSC track segment (useful for low-p_{T} muons).
- Calo Tagged (CT): The ID track is extrapolated to the calorimeter, where it matches an energy deposit (useful in the region $|\eta| < 0.1$ where the MS has no coverage).
- Stand Alone (SA): A MS track not matched to an ID track, but extrapolated close to the IP, is used to recover muons in the range $2.5 < |\eta| < 2.7$ that has poor ID coverage.

For muon identification, “Medium” working point only uses CB and SA candidates, while the “Loose” working point considers all four types.

Energy Clusters

Calo-clusters

- Electron objects are reconstructed by matching clusters of EM calorimeter energy deposits to reconstructed tracks in the ID
- Sliding window algorithm:
  - Window: fixed-size grid of cells, $N_\eta \times N_\phi = 3 \times 5$, in middle layer of the LAr calorimeter ($80\,\%$ of energy in EM shower deposited)
  - For each cell, energy is summed across all longitudinal layers, forming a tower. If transverse energy of towers in window is above 2.5 GeV and local max, seed cluster formed
- If cluster matches ID track, cluster rebuilt by summing energy in grid of 3×7 cells in each layer, starting in middle layer.

Topo-clusters

- Hadronization of quarks from hard scatter event, or subsequent hadronic decays of unstable particles ($W/Z \rightarrow q\bar{q}'$), creates showers of lower energy particles, called jets, in the detector.
- Jets formed by clustering nearby energy deposits in the calorimeter and matching the cluster with ID tracks
- "Topo-clusters": topologically connected three dimensional cell clusters (variable sized)
- Topo-cluster seeded if energy of cell is four standard deviations above noise level ($E_{\mathrm{cell}} > 4\sigma^{\mathrm{noise}}_{\mathrm{cell}}$)
- Connected cells are added to cluster if $E_{\mathrm{cell}} > 2\sigma^{\mathrm{noise}}_{\mathrm{cell}}$

Jets - Anti-k_T Algorithm

- Anti-k_T jet reconstruction algorithm is a sequential combination algorithm used to combine topo-clusters into jet objects
- Distances defined: d_{ij} between constituents (clusters); d_{iB} between cluster and beam line

$$d_{ij} = \min\left(\frac{1}{p_{\mathrm{T,i}}^2}, \frac{1}{p_{\mathrm{T,j}}^2}\right)\frac{\Delta R_{ij}^2}{R^2}$$

$$d_{iB} = \frac{1}{p_{\mathrm{T,i}}^2}$$

- Distance parameter R roughly defines the size of the jet
- Clustering procedure iteratively finds smallest distance among all constituents
  - If smallest distance is between two clusters, d_{ij}, clusters are combined and procedure continues
  - If between a cluster and beam axis, d_{iB}, cluster is defined as a jet and removed from collection of remaining constituents
- Distances are recalculated, more jets are formed until no remaining clusters
- Algorithm tends to combine high-p_T constituents first, produces roughly conical jet

Jet b-tagging

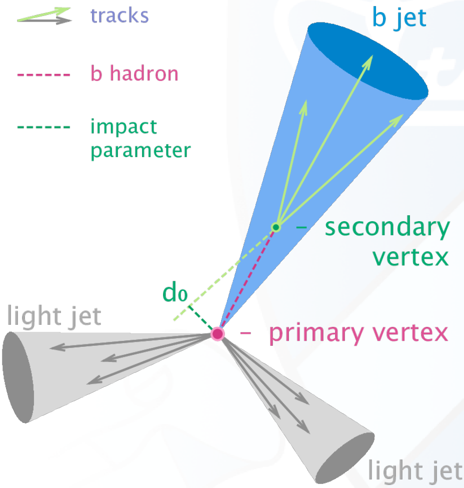

- Life time of hadrons with b-quarks long enough for displacement
- Short enough to differentiate from hadrons with light-quarks
- Find secondary vertices
- Look for decay products (higher multiplicities, low energy leptons with p_{T}, etc)
- Reconstruct decay chain

Large-R Jets - Combined Mass

- Jet mass resolution can suffer in the high-p_{T} regime from loss of angular information when multiple highly boosted decay products are reconstructed as a single topo-cluster
- m_{track}, calculated by ghost associating ID tracks with $p_{\mathrm{T}} > 0.4$ GeV to large-R jet, summing masses of all matched tracks
    - Ghost association: tracks identified as particles with infinitesimal momentum, included in clustering process. Their negligible momentum ensures final jet clusters are not affected, but will include the tracks
- m_{TA} (track-assisted): correct for missing neutral particle contribution to m_{track}, use ratio of calorimeter-based to track-

- $m_{\mathrm{TA}} \equiv m_{\mathrm{track}} \times \frac{p_{\mathrm{T}}^{\mathrm{calo}}}{p_{\mathrm{T}}^{\mathrm{track}}}$
- Combined mass: weighted sum, minimizing the jet mass resolution (take advantage of both m(TA) and m(calo) – assumed uncorrelated). Jet transverse momentum also re-scaled to be compatible with combined mass:

$$m_{\mathrm{comb}} \equiv w_{\mathrm{calo}} \times m_{\mathrm{calo}} + w_{\mathrm{track}} \times m_{\mathrm{TA}}$$
$$p_{\mathrm{T}}^{\mathrm{comb}} \equiv p_{\mathrm{T}}^{\mathrm{calo}} \times \frac{m_{\mathrm{comb}}}{m_{\mathrm{calo}}}$$

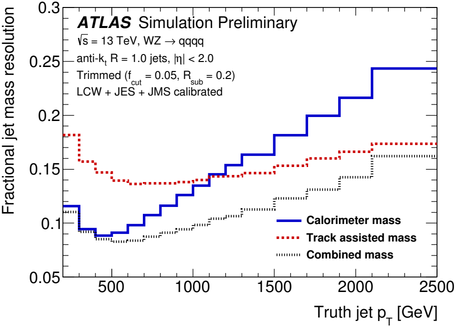

Large-R Jets - Substructure ($D_2^{\beta=1}$)

- Jets from two-body decays of boosted vector bosons have a substructure typically absent from decays of gluons and light quarks
- Substructure variable, $D_2^{\beta=1}$, based on ratio of two and three point energy correlation functions:
- $e_2^{\beta} = \frac{1}{p_{\mathrm{T}}^2(J)} \sum_{1 \leq i < j \leq n_j} p_{\mathrm{T}}^i p_{\mathrm{T}}^j \Delta R_{ij}^{\beta}$
  $e_3^{\beta} = \frac{1}{p_{\mathrm{T}}^2(J)} \sum_{1 \leq i < j < k \leq n_j} p_{\mathrm{T}}^i p_{\mathrm{T}}^j p_{\mathrm{T}}^k \Delta R_{ij}^{\beta} \Delta R_{ik}^{\beta} \Delta R_{jk}^{\beta}$
  $D_2^{\beta=1} = \frac{e_3^{\beta=1}}{\left(e_2^{\beta=1}\right)^3}$
- For n_j constituents in jet, p_{T}^i is transverse momentum of $\mathrm{i^{th}}$ constituent, and ΔR_{ij} is angular separation between $\mathrm{i^{th}}$ and $\mathrm{j^{th}}$ constituents.
- Signal-like jets will have lower values of $D_2^{\beta=1}$, upper-cut is used in the boson-tagger

Missing Transverse Energy ($E_{\mathrm{T}}^{\mathrm{miss}}$)

- Protons have no initial momentum transverse to the beam line $\Rightarrow$ vector sum of transverse momentum of all final state particles should also be zero (momentum conservation)
- Deviations from zero can indicate the presence of a non-interacting particle, like a neutrino, in the final state (Neutrinos pass through ATLAS without leaving energy deposits in calorimeters, or tracks in the ID and MS.)
- $E_{x(y)}^{\mathrm{miss}} = -\sum_{e \in \{\mathrm{electrons}\}} p_{x(y)}^{e} - \sum_{\mu \in \{\mathrm{muons}\}} p_{x(y)}^{\mu} - \sum_{j \in \{\mathrm{jets}\}} p_{x(y)}^{j} - \sum_{s \in \{\mathrm{soft\ terms}\}} p_{x(y)}^{s}$

  $E_{\mathrm{T}}^{\mathrm{miss}} = \sqrt{(E_x^{\mathrm{miss}})^2 + \left(E_y^{\mathrm{miss}}\right)^2}$
- Negative vector sum of all reconstructed objects, and additional "soft terms" corresponding to tracks from PV that are not matched to reconstructed objects
- Track-based soft terms ignore possible contributions from neutral particles, calo-based soft term can be used but has poorer $E_{\mathrm{T}}^{\mathrm{miss}}$ resolution and more pileup-dependent
- Photons and hadronically decaying taus are not used in this analysis, reconstructed as jets in the $E_{\mathrm{T}}^{\mathrm{miss}}$ calculation.

Overlap Removal

- Single collection of energy deposits and tracks may be reconstructed independently as several physics objects
- If shared ID track between e/μ candidate, e removed. MS track cannot be due to e.
- If $\Delta R(j, e) < 0.2$, small-R jet removed - reconstructed jet does not differentiate between had/EM showers.
  - Electron removed if $0.2 < \Delta R(j, e) < \min(0.4, 0.04 + 10\,GeV/p_{\mathrm{T}}(e))$. Electrons reconstructed near jet edge most likely from non-prompt decays of jet constituents. Sliding cone, with max size $R = 0.4$ at low $p_{\mathrm{T}}(e)$, recovers boosted prompt electrons that are close jet edge
- If $\Delta R(J, e) < 1.0$, large-R jet removed
- If $\Delta R(j, \mu) < 0.2$, and either 1) jet has fewer than two tracks or 2) $p_{\mathrm{T}}(\mu)/p_{\mathrm{T}}(j) > 0.5$ and $p_{\mathrm{T}}(\mu)/\sum p_{\mathrm{T}}(\mathrm{tracks}) > 0.7$, jet is discarded. Indicates jet most likely from calorimeter energy loss of a muon.
  - If jet not removed, sliding cone used to remove muon if $\Delta R(j, \mu) < \min(0.4, 0.04 + 10\,GeV/p_{\mathrm{T}}(\mu))$. Boosted muons sufficiently far from jet center kept, lower p_{T} muons likely from non-prompt decays near jet edge removed.
- No overlap removal between muons and large-R jets, muons are unlikely to deposit enough calorimeter energy to be reconstructed as a jet with $p_{\mathrm{T}} > 200$ GeV.

Signal and Background Modeling

- Monte Carlo (MC) techniques used to model both sig. and bkg. processes
- LHC collisions involve both hard (perturbative QCD) and soft (non-perturbative QCD) processes
- Calculation split into "matrix element" (hard scatter interaction) and parton showering (subsequent hadronization of fragmented partons) steps
- Matrix element step: fixed number of incoming/outgoing particles, calculated at LO and NLO in α_S
- "Underlying event" (UE) overlaid
  - Processes not originating from hard scatter event
  - Includes ISR/FSR, additional interactions of fragments of colliding protons
- PYTHIA 8.186 used for modeling pile-up
- Simulated events propagated through detector using GEANT4, reconstructed with standard ATLAS software

MC Generators

- $2 \rightarrow 2$ generators: PYTHIA, HERWIG++, POWHEG
  - Model exactly two incoming and two outgoing particles
  - PYTHIA and HERWIG++ are capable of additionally modeling showering process
- $2 \rightarrow n$ generators: SHERPA, MADGRAPH
  - Same jet multiplicity possible at matrix element and showering stage, careful of double counting
  - SHERPA uses own showering
  - MADGRAPH useful for new physics models
- Parton Distribution Functions (PDF):
  - MC generators use PDFs to model partons in interaction
  - Probability that a certain parton with a specified momentum fraction exists in the initial protons
- MADGRAPH used for HVT and RS G^*, POWHEG used for heavy Higgs
- SHERPA v2.1.1 used for $W/Z + jets$ and SM dibosons, POWHEG used for $t\bar{t}$ and single-t
- Generators for all bkg processes use cross sections determined at NNLO, except diboson samples which use NLO cross sections from generator.

Event Preselection

- Good Runs List: data from periods of time (lumi-blocks) where detector fully operational, and of adequate quality (stable beams, magnets on, subdetectors on, few noisy cells)
- Primary Vertex: require primary vertex with at least two tracks, each with $p_{\mathrm{T,trk}} > 400$ MeV (largest $\sum p^2_{\mathrm{T,trk}}$ selected)
- Subdetector Error Veto: corrupted events from LAr/Tile/SCT vetoed (also if close to noise burst LAr)
- Incomplete Events: rejected if missing detector information
- Bad Jet Veto: Noise bursts or coherent noise in calorimeters, hardware issues, beam backgrounds, and cosmic muons can create fake jets. A high efficiency working point, called BadLoose, is defined to reject events with "bad" jets. These bad jets can degrade the calculation of $E_{\mathrm{T}}^{\mathrm{miss}}$. Since e/μ can be reconstructed as bad jets, overlap removal between signal and veto leptons and jets is applied before bad jet veto.
- Second Lepton Veto: exactly one lepton, no "veto" leptons.
- Signal lepton: pass signal lepton definition.
- Trigger Matching: reconstructed signal lepton must match physics object that passed trigger

Event Reweighting

- Generated MC samples require various weights to match distribution observed in data
- Weights applied for: pile-up reweighting, eff. of reconstructed objects MC/data, lepton reconst./iso. eff., electron ID/trigger matching, eff of associating muon tracks to a vertex, *b*-tagging eff.
- MC scaled to measured integrated lumi, take into account higher order corrections to cross sections and filter eff. (enforcing specific final state)

Regulating Jet Production

- Protons in collision have substructure
- Scattering
  - Hard: perturbative QCD (e.g. W production)
  - Soft: low momentum transfer (e.g. pile-up), non-perturbative
- Factorization theorem: cross section for collision of two protons
  - Includes terms for LO, NLO and PDFs
  - Cross section factorized into hard part and normalization from PDFs
  - Two scales: factorization/renormalization
- Resummation: analytical extraction of leading logarithms (NLL etc.)
  - Accounts for enhanced set of terms at every order in perturbative series
- Affect production of jets

Binned Maximum Likelihood (ML) Fit

- $P(n_{\mathrm{obs}}|n_{\mathrm{exp}}) = \frac{(n_{\mathrm{exp}})^{n_{\mathrm{obs}}} e^{-n_{\mathrm{exp}}}}{n_{\mathrm{obs}}!}$
  $L(\mu, \theta) = \prod_{j \in \{\mathrm{SRs,\ CRs}\}} \prod_{i \in \{\mathrm{bins}\}} P(N_{ij}|\mu s_{ij} + B_{ij}) \prod_{l \in \{\mathrm{NPs}\}} \mathrm{Nuis}(\theta_l)$
  $B_{ij} = \mu_{t\bar{t}} b_{ij}^{t\bar{t}} + \mu_{W+\mathrm{jets}} b_{ij}^{W+\mathrm{jets}} + b_{ij}^{\mathrm{other}}$

- Simultaneous binned ML fit of the $m(\ell\nu J)$ distribution in the SRs and CRs is performed on MC to data.
- WW and WZ analyzed separately (large overlap); additionally, VBF and ggF selections fit separately
- Models with ggF (or qqF) production are analyzed with fit to ggF selection, while models with VBF production are analyzed with fit to VBF selection
- For each fit, there is a common normalization factor for HP and LP regions, for each of two main backgrounds (W+jets and $t\bar{t}$). Normalizations are free to float in fit, and constrained by the CRs

- Signal strength (μ) parameterizes production of signal events: $\mu = 1$ is nominal signal hypothesis, $\mu = 0$ is bkg-only hypothesis.
- θ represents collection of all NPs.
- In likelihood function, index j runs over SRs/CRs in fit; index i runs over bins of $m(\ell\nu J)$ distribution in each region; index l runs over all NPs considered.
- For each bin i and region j, N_{ij}, is number of observed data events, s_{ij} is number of expected signal events, and B_{ij} is number of expected background events.
- In B_{ij}, $\mu_{t\bar{t}}$ (μ_{W+jets}) is normalization factor for $t\bar{t}$ (W+jets) bkg, and b_{ij}^{x} is expected number of bkg events for bkg process x (i.e. $t\bar{t}$, W+jets, or other = single-t, Z+jets, and SM dibosons).

Binning

Binning

- Variable binning optimized to HVT Z' signal resolution, enlarged in high mass region to ensure sufficient entires in each bin
- 20 (11) bins used for ggF (VBF) selection

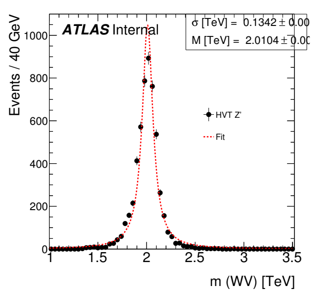

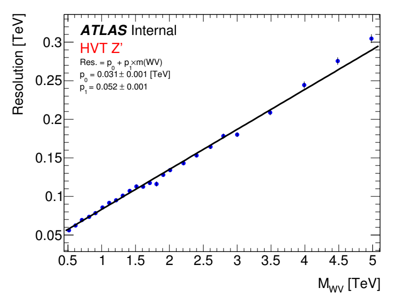

Signal Mass [TeV]	HVT Z'		RSG G^*	
	$\Gamma_{\text{exp.}}$ [GeV]	$\Gamma_{\text{meas.}}$ [GeV]	$\Gamma_{\text{exp.}}$ [GeV]	$\Gamma_{\text{meas.}}$ [GeV]
0.8	32	74	46	90
1.6	51	113	96	149
2.4	74	153	148	238

Nuisance Parameters

- Systematic uncertainties included as constrained NPs in fit with Gaussian or log-normal constraints, centered at 0 with width 1
- For each systematic uncertainty, "up" and "down" histograms are generated, corresponding to variation of systematic uncertainty by $\pm 1\sigma$
- Impact of systematic uncertainty on nominal event yield is parameterized by a NP, θ, such that $\theta = \pm 1$ corresponds to variation of systematic uncertainty by $\pm 1\sigma$
- Event yield is factored according to separate contributions from each NP, $(\mu s + B)^{\pm,\, 0}$ corresponds to event yield from "up" (+), "down" (−), or nominal (0) variations
- $\mu s + B = (\mu s + B)^0 \prod_l (1 + \Delta_l \theta_l)$

$$\Delta_l = \begin{cases} \frac{(\mu s + B)^+ - (\mu s + B)^0}{(\mu s + B)^0} & \theta_l \geq 0 \\ \frac{(\mu s + B)^0 - (\mu s + B)^-}{(\mu s + B)^0} & \theta_l < 0 \end{cases}$$

- For each NP, correlations are taken into account between bins in final discriminant, between regions in fit, and between bkg and signal distributions
- For some systematic uncertainties, estimated variations used MC with limited statistics. To lessen effect of statistical fluctuations, some variations of systematic uncertainties smoothed.
- Event yield in bin i for "up" or "down" histogram of smoothed systematic uncertainty is set according to:

$$(\mu s + B)_i^{\pm} = (\mu s + B)_i^0 \left[1 + \lambda_i^{\pm}\right]$$

$$\lambda_i^{\pm} = \frac{1}{4}\Big(\left[(\mu s + B)_{i-1}^{\pm} - (\mu s + B)_{i-1}^0\right] + 2\left[(\mu s + B)_i^{\pm} - (\mu s + B)_i^0\right] + \left[(\mu s + B)_{i+1}^{\pm} - (\mu s + B)_{i+1}^0\right]\Big)$$

Profile Log Likelihood (PLL) Ratio - Upper Limits

- With no significant excesses observed in the ML fit (bkg-only hypothesis), upper limits on cross section set using test statistic, $\tilde{q_\mu}$, based on PLL ratio

- $$\tilde{\lambda}(\mu) = \begin{cases} \frac{L(\mu,\hat{\hat{\theta}}(\mu))}{L(\hat{\mu},\hat{\theta})} & \hat{\mu} \geq 0 \\ \frac{L(\mu,\hat{\hat{\theta}}(\mu))}{L(0,\hat{\hat{\theta}}(0))} & \hat{\mu} < 0 \end{cases}$$
  $$\tilde{q}_\mu = \begin{cases} -2\ln\tilde{\lambda}(\mu) & \hat{\mu} \leq \mu \\ 0 & \hat{\mu} > \mu \end{cases}$$
- $\hat{\hat{\theta}}(\mu)$ is value of θ that maximizes likelihood function, L, for a fixed value of μ. This is conditional ML estimator of θ, and is a function of μ.
- The denominator is the ML function; that is, $\hat{\mu}$ and $\hat{\theta}$ are the unconditional ML estimators of μ and θ.
- Value of estimator, $\hat{\mu}$, that maximizes likelihood function is allowed to be negative so it can be modeled by a Gaussian distributed variable.

- If $\hat{\mu} < 0$, denominator in PLL ratio is fixed to physical value that best describes data – with $\mu = 0$ and $\hat{\hat{\theta}}(\mu = 0)$.
- $\tilde{\lambda}$ constrained $0 \leq \tilde{\lambda} \leq 1$; closer to 1 indicate better agreement between data and hypothesized signal strength, μ
- $\tilde{q}_\mu$: larger values indicate less compatibility between data and hypothesized signal strength
- If $\hat{\mu} > \mu$, $\tilde{q}_\mu = 0$ – an estimated $\hat{\mu}$ larger than hypothesized value does not represent lower compatibility with data, not part of the region rejected by one-sided upper limit

Upper Limits - CL_s Method

- p-value calculated from probability distribution function (PDF) of test statistic, $f(\tilde{q}_\mu|\mu) \Rightarrow \quad p_\mu = \int_{\tilde{q}_{\mu,\,\mathrm{obs}}}^{\infty} f(\tilde{q}_\mu|\mu) d\tilde{q}_\mu$
- Asymptotic distributions of $f(\tilde{q}_\mu|\mu)$ for masses below 1.6 TeV (1.0 TeV) for ggF (VBF) selection. Higher masses, PDFs estimated with 50k generated pseudo-experiments using toy MC methods (good agreement in transition region, more conservative at higher masses).
- Modified frequentist approach, called the CL_s method, employed to set final upper limits: uses ratio of two frequentist confidence levels (CL)
- $CL_s = \frac{CL_{s+b}}{CL_b} = \frac{p_{s+b}}{1-p_b}$
  $p_{s+b} = \int_{\tilde{q}_{\mu,\,\mathrm{obs}}}^{\infty} f(\tilde{q}_\mu|\mu) d\tilde{q}_\mu$
  $1 - p_b = \int_{\tilde{q}_{\mu,\,\mathrm{obs}}}^{\infty} f(\tilde{q}_\mu|\mu = 0) d\tilde{q}_\mu$
- Values of CL_{s+b} close to zero indicate the signal model is highly disfavored.
- Model with signal strength, μ, excluded if $CL_s < 0.05$, (CL of 95 %)
- 95 % CL upper limit is set by scanning and finding μ^{up} such that $CL_s = 0.05$
- p_{s+b}: (sig. plus bkg. hyp., with μ) prob of measuring $\tilde{q}_\mu$ equally or less compatible with tested signal strength than $\tilde{q}_{\mu,\,\mathrm{obs}}$.
- $1 - p_b$: (bkg-only hyp.) prob of measuring $\tilde{q}_\mu$ greater than or equal to value observed $\Rightarrow$ prob. to correctly reject the tested value of μ when bkg-only hyp. correct
- CL_s method conservative (wrt true frequentist CL): $1 - p_b \leq 1 \Rightarrow CL_s < 0.05$ is more stringent than $p_{s+b} < 0.05$.
- In CL_s, p-value penalized in regions where no sensitivity: PDFs of test statistic for sig + bkg model and bkg-only model will have a large overlap $\Rightarrow$ as p_{s+b} decreases so does $(1 - p_b)$, preventing $CL_s < 0.05$.

Fit Results

Normalization Factors

- Normalization factors for the W+jets and $t\bar{t}$ backgrounds for the WW and WZ channels, separated into ggF and VBF selections. The normalization factor is the ratio between the number of fitted events from simulation to the number of predicted events from simulation. The uncertainties include both statistical and systematic uncertainties.

Bkg.	WW Selection		WZ Selection	
Norm.	ggF	VBF	ggF	VBF
W+jets	0.95 ± 0.06	0.89 ± 0.18	0.97 ± 0.06	0.84 ± 0.16
$t\bar{t}$	1.03 ± 0.06	1.21 ± 0.18	1.00 ± 0.06	1.10 ± 0.17

Impact of NP on Fit

- Relative change in signal strength ($\Delta\hat{\mu}$) with respect to the best-fit value after the fit to data. The five dominant uncertainty sources are presented for the ggF and VBF selections, along with the effect of the data statistical uncertainties. These are evaluated from the 2 TeV (1.2 TeV) mass point for the ggF (VBF) selection. To evaluate the impact on μ, the production cross section is assumed the be the expected upper limit at the mass point.

ggF Selection (Impact on μ)		VBF Selection (Impact on μ)	
Source	$\Delta\hat{\mu}/\mu$ (%)	Source	$\Delta\hat{\mu}/\mu$ (%)
	$m(WZ) = 2000$ GeV		$m(WW) = 1200$ GeV
W+jets modeling MadGraph	8	Large-R jets mass resolution	5
W+jets modeling scale	5	W+jets PDF	5
SM diboson normalization	4	Top modeling Herwig	5
Large-R jets mass resolution	4	W+jets normalization	5
Large-R jets D_2 resolution	4	Top modeling radiation	4
Total systematic uncertainties	20	Total systematic uncertainties	24
Data statistics	50	Data statistics	52

Post fit (VBF Selection)

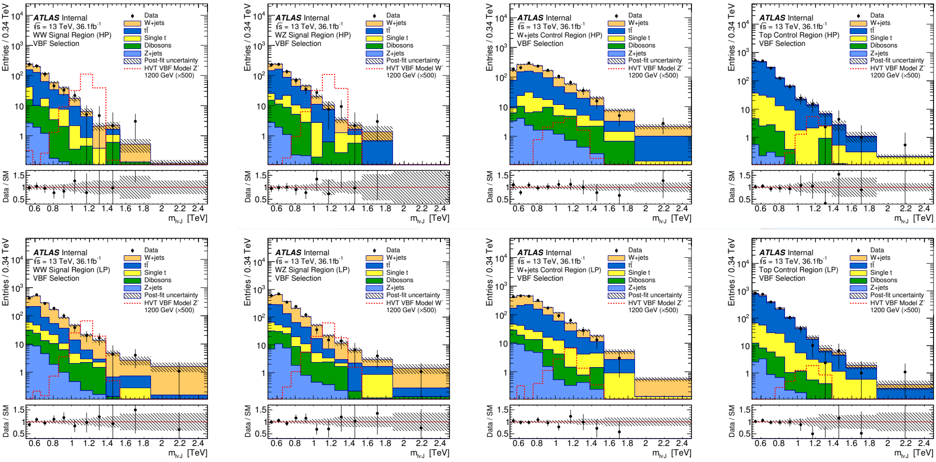

Post fit (ggF Selection)

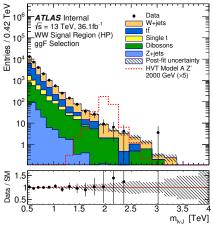

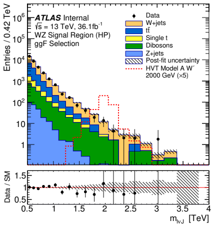

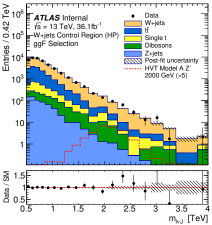

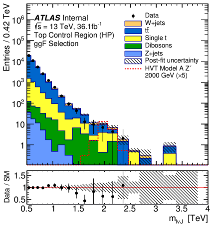

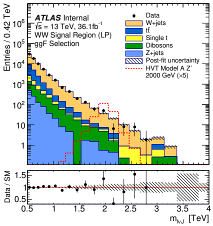

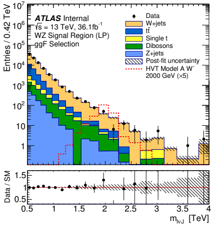

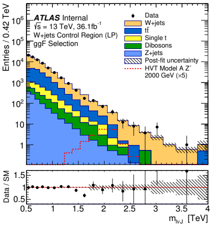

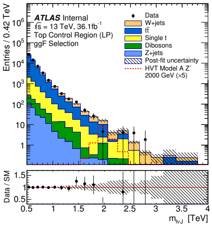

Upper Limits

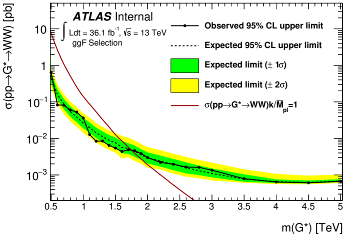

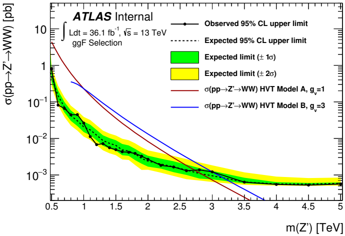

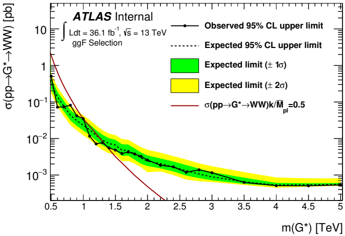

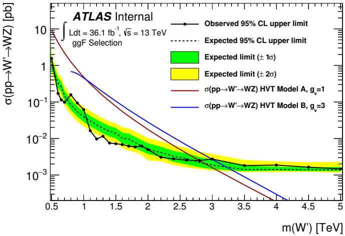

The observed and expected 95% CL upper limits on cross section times branching ratio for HVT Z'/W' and RS G^* in the combined LP and HP signal regions, for the ggF selection. The theoretical cross sections for model-A/B are overlaid for HVT, $k/\overline{M}_{\mathrm{Pl}} = 0.5, 1.0$ for G^*. Limits are calculated with an asymptotic approximation for mass points below 1.6 TeV, and with pseudo-experiments above 1.6 TeV.

Upper Limits

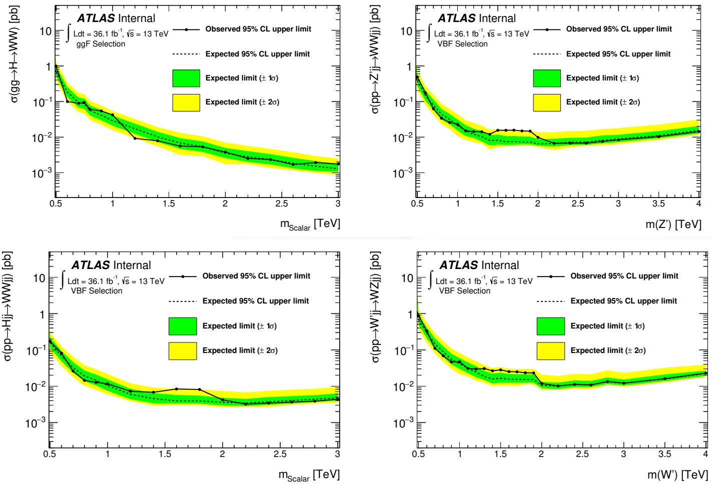

The observed and expected 95 % CL upper limits on cross section times branching ratio for HVT W'/Z' and neutral heavy scalar (NWA), in the combined LP and HP signal regions, for the VBF selection (and ggF for scalar model). Signal samples generated with ggF (VBF) production are used for the ggF selection (VBF selection). The mass region greater than 1.5 TeV is covered by two bins in the final discriminant, while the observed limit markers represent the tested signal points. For the ggF (VBF) selection, limits are calculated with an asymptotic approximation for mass points below $1.6\,TeV$ $(1.0\,TeV)$, and with pseudo-experiments above $1.6\,TeV$ $(1.0\,TeV)$.